



Contents lists available at ScienceDirect

Journal of Volcanology and Geothermal Research

journal homepage: www.elsevier.com/locate/jvolgeores

Kaguyak dome field and its Holocene caldera, Alaska Peninsula

Judy Fierstein*, Wes Hildreth

U.S. Geological Survey, Volcano Hazards Team/MS-910, 345 Middlefield Road, Menlo Park, CA 94025, USA

ARTICLE INFO

Article history:

Received 3 December 2007

Accepted 16 May 2008

Available online xxx

Keywords:

Kaguyak caldera

lava domes

ignimbrite

caldera-forming eruption

Aleutian arc volcano

ABSTRACT

Kaguyak Caldera lies in a remote corner of Katmai National Park, 375 km SW of Anchorage, Alaska. The 2.5-by-3-km caldera collapsed $\sim 5.8 \pm 0.2$ ka (^{14}C age) during emplacement of a radial apron of poorly pumiceous crystal-rich dacitic pyroclastic flows (61–67% SiO_2). Proximal pumice-fall deposits are thin and sparsely preserved, but an oxidized coignimbrite ash is found as far as the Valley of Ten Thousand Smokes, 80 km southwest. Postcaldera events include filling the 150-m-deep caldera lake, emplacement of two intracaldera domes (61.5–64.5% SiO_2), and phreatic ejection of lakefloor sediments onto the caldera rim. CO_2 and H_2S bubble up through the lake, weakly but widely. Geochemical analyses ($n=148$), including pre- and post-caldera lavas (53–74% SiO_2), define one of the lowest-K arc suites in Alaska. The precaldere edifice was not a stratocone but was, instead, nine contiguous but discrete clusters of lava domes, themselves stacks of rhyolite to basalt exogenous lobes and flows. Four extracaldera clusters are mid-to-late Pleistocene, but the other five are younger than 60 ka, were truncated by the collapse, and now make up the steep inner walls. The climactic ignimbrite was preceded by ~ 200 years by radial emplacement of a 100-m-thick sheet of block-rich glassy lava breccia (62–65.5% SiO_2). Filling the notches between the truncated dome clusters, the breccia now makes up three segments of the steep caldera wall, which beheads gullies incised into the breccia deposit prior to caldera formation. They were probably shed by a large lava dome extruding where the lake is today.

Published by Elsevier B.V.

1. Introduction

Kaguyak is a young silicic volcanic center with a 2.5-by-3-km-wide lake-filled Holocene caldera that lies in the remote NE corner of Katmai National Park on the Alaska Peninsula, 375 km SW of Anchorage (Figs. 1, 2). Although the caldera was long recognized to be postglacial, little was known about the volcano itself prior to this investigation, and the precaldere edifice was widely assumed to have been a single stratocone (Wood and Kienle 1990; Riehle et al. 1996). Our mapping shows, instead, that it consists of nine contiguous but discrete clusters of lava domes, each a stack of andesitic to rhyolitic exogenous lobes and flows (Fig. 3). Five dome clusters were truncated by the Holocene collapse and now make up the steep inner walls of the caldera. The longest-lived includes flows as old as ~ 300 ka and as young as 50 ka, but the other four are all younger than 60 ka. Four extracaldera clusters are mid-to-late Pleistocene, and two additional domes are postcaldera, the smaller of which forms a small island in the middle of the caldera lake. The collapse itself was accompanied by a moderate-sized ignimbrite that flowed 15 km to the sea. The caldera-forming eruption was shortly preceded by a catastrophic dome destruction that resulted in radial emplacement of a coarse dacite breccia deposit subsequently cut by the caldera.

1.1. Methods

Three weeks of field work included a week of mapping the steep caldera walls in detail, with access by inflatable boat from a bear-safe camp on the small intracaldera island. The area is uninhabited and there are no roads. All supplies, including the boat, were brought in by float plane from the closest town, King Salmon, 140 km to the west (Fig. 1). Although the postglacial outflow deposits are moderately well preserved, coastal Alaskan brushy vegetation limits exposure. It also provides cover for brown bears, which are common enough to have beaten a path circumambulating the entire caldera rim (even its craggy summits); as many as 25 bears at a time were seen grazing together along the coastal shoreline. Thus, in large part for safety, mapping the volcano flanks and pyroclastic outflow sheet was done by helicopter based out of King Salmon. These efforts yielded a sample from virtually every eruptive unit exposed in the caldera walls, from all the extracaldera domes, and a representative suite from the extensive pyroclastic outflow.

The mapping and sampling are the basis for the eruptive history presented below, from oldest to youngest. There are significant hazards considerations not only because the Holocene caldera is not far from population centers on Cook Inlet and Kodiak Island, but because Kaguyak has been a silicic focus for several hundred thousand years. The age of the caldera, previously inferred only by indirect evidence, is now well established by regional tephra studies and ^{14}C dating (Fierstein, 2007), and by proximal stratigraphic relations discussed below.

* Corresponding author. Tel.: +1 650 329 5202; fax: +1 650 329 5203.

E-mail addresses: jfierstn@usgs.gov (J. Fierstein), hildreth@usgs.gov (W. Hildreth).

Kaguyak lavas have been dated by $^{40}\text{Ar}/^{39}\text{Ar}$ and K–Ar methods in the Menlo Park U.S. Geological Survey geochronology laboratory. Despite success in dating young volcanic rocks elsewhere (e.g., Calvert et al., 2003), many of our experiments at Kaguyak have proven imprecise owing to the low potassium content of the rocks. Results that seem analytically reliable and in accord with field relations are presented below in order to provide a first-order time-stratigraphic framework for the center. A more complete treatment of the geochronologic results will be published separately. Radiocarbon ages presented here were all determined at Geochron Laboratories in

Cambridge, MA and include dates on humic acids in soils and on charred twigs in fall and flow deposits. All are stated in terms of uncalibrated ^{14}C years B.P.; a more complete discussion of the analytical methods, calibrated ages, and preferred ages based on geologic evidence is given in Fierstein (2007).

Descriptions of the lavas include petrographic comparisons in which we use mineral-name abbreviations for plagioclase (pl), orthopyroxene (opx), clinopyroxene (cpx), olivine (ol), hornblende (hb) and magnetite (mt). We use ‘basalt’ for the few lavas that have ~53% SiO_2 , ‘andesite’ 54–63% SiO_2 , ‘dacite’ 63–68% SiO_2 , ‘rhyodacite’

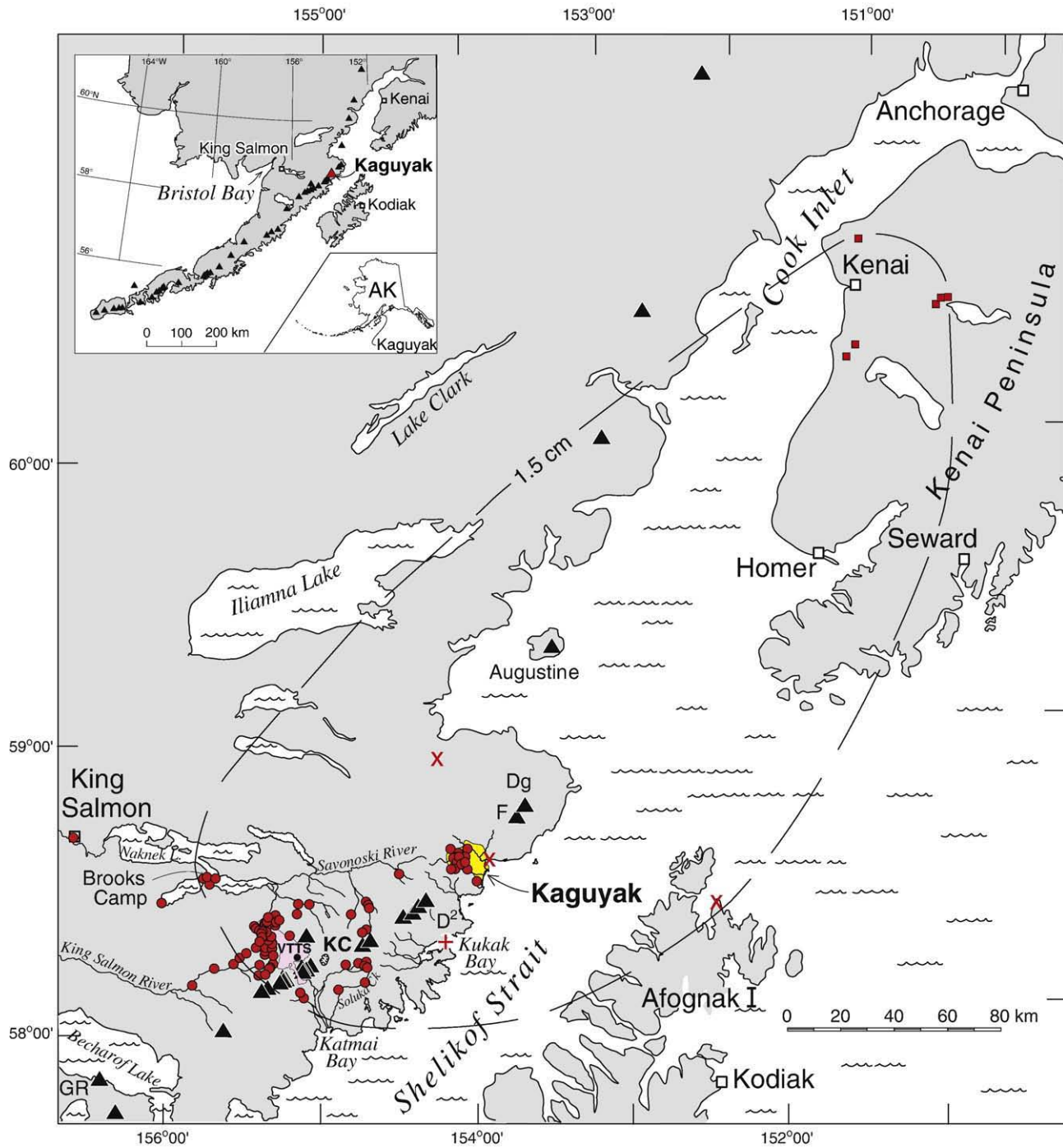


Fig. 1. Location map showing the 475-km-long stretch of the Aleutian Arc SW and NE of Kaguyak caldera. Probable original extent of the Kaguyak ash-flow sheet in yellow. Labeled elliptical curve is the approximate 1.5-cm isopach for the (largely coignimbrite) fallout from the caldera-forming eruption. Filled red circles are our measured tephra sites; red squares are sites from Reger et al. (1996); red X's from Riehle et al. (1999); red (+) near Kukak Bay from Nowak (1968); see Section 8 for discussion of thickness measurements. Valley of Ten Thousand Smokes ash-flow sheet (VTTS) is pink; Novarupta (filled circle) is at its head. Volcanoes (filled triangles) mentioned in text are labeled: Douglas (Dg); Fourpeaked (F); Devils Desk (D²); Katmai caldera (KC); Gas Rocks (GR).

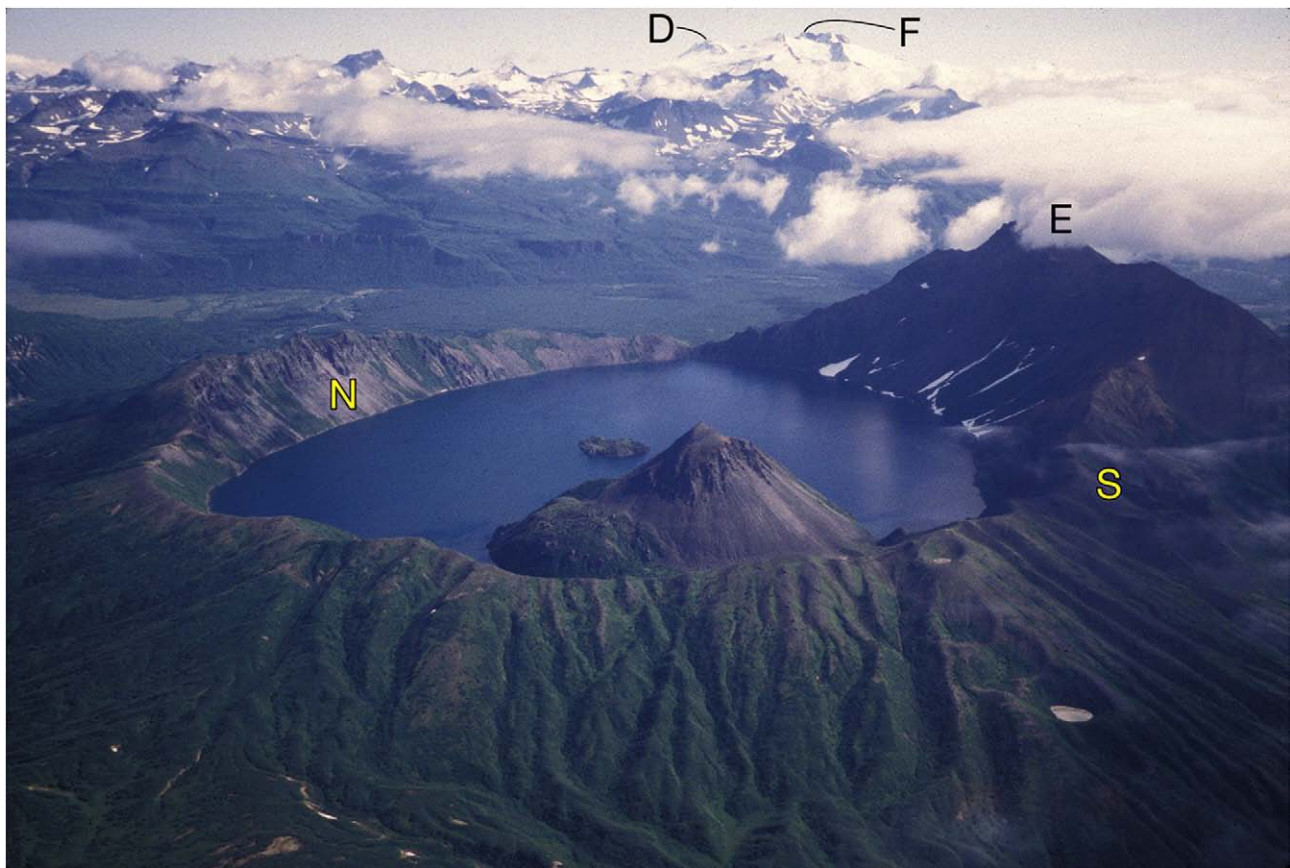


Fig. 2. Aerial view northeastward of Kaguyak caldera filled with a 150-m-deep lake. One large, composite post-caldera dome impinges on the SW wall; the most recent dome shows only as a small island in the middle of the lake. Steep caldera walls expose the broad Northern Edifice (N; left) and tallest Eastern Edifice (E; right, summit in cloud). Radial rivulets cut in the Big Breccia deposit (seen here in the foreground around the rim) were beheaded by the caldera-forming event. A line of four explosion pits (lower right) cut the Breccia deposits and strike NNE directly toward the two post-caldera domes. Low point on the rim between Northern and Eastern Edifices is the northeast notch. Low point on the rim on the other side of the Eastern Edifice is the southern saddle, where remnants of the Southern Edifice (S) overlap the Eastern (far right, center). Lowland beyond the caldera is the glaciated Big River valley (see Fig. 3), once filled by the Kaguyak ignimbrite. Flat-topped bench just beyond the river is Jurassic sedimentary basement capped by a few remnants of what we think are Kaguyak lavas. Tall distant snowy peaks (central skyline) are Mount Douglas (D) Fourpeaked volcano (F).

69–72% SiO₂, and ‘rhyolite’ ≥ 73% SiO₂. Samples are all numbered “Y-1, Y-2”, etc., throughout the text. We begin by describing the precaldra dome clusters (Eastern, Southern, and Northern Edifices), as well as remnants of several other lava flows and domes, all of which are exposed in the caldera walls. This is followed by description of the explosive emplacement of the Big Breccia and succeeding ignimbrite with attendant caldera formation and the postcaldera domes. Described next are the extracaldra domes, all precaldra but not exposed in the caldera walls, and is followed by discussion of the chemistry and gas seeps in the caldera lake. We close with a synthesis of the eruptive history of the Kaguyak dome field, including discussion of volumes, spatial development, and compositional changes through time.

2. Eastern Edifice

Highest, largest, and oldest of the dome complexes, the Eastern Edifice is 2956 ft. in elevation at its highest point, its caldera-wall exposures rising steeply 1756 feet (532 m) above the caldera lake (Fig. 4). At least ten units (61%–71% SiO₂) are grouped into four packages likely to have erupted in coherent episodes. Constructed of several lava flow lobes emplaced atop older domes, the Eastern Edifice extends from the NE notch to the southern saddle (Figs. 2–4), forming about a third of the inner caldera wall. Its lavas are compositionally distinguished from other caldera-wall edifices by higher Ca and Mg and lower Fe and Ti (Fig. 5, Appendix C), petrographically by smaller plagioclase phenocrysts (typically 1–2 mm) and the absence of hornblende, and include some of the most silicic products erupted at Kaguyak.

2.1. Eruptive package 1: oldest lavas at lakeshore

The oldest eruptive package exposed in the caldera wall is made up of two separate domes along the lakeshore, both of which are Fe-stained, pervasively acid-altered, and locally include pyrite crystals. The older of the two, dated at 301 ± 65 ka (Y-31, Fig. 4; Table 1), is exposed only as a small 15-m-high cliffy outcrop enveloped by talus just above the eastern shoreline near the NE notch (Fig. 4). One of the few rhyodacites at Kaguyak (70.5% SiO₂), it is the most silicic unit exposed on the caldera walls (Figs. 5, 6). The other dome (~65% SiO₂)—similarly rusty orange and altered—is a dacite as much as ~300 m thick where it makes up two-thirds of the caldera wall and much of the saddle on the south rim. Internally greenish-grey and intricately jointed into thin plates and chunks, the lava is phenocryst-poor relative to all other units exposed in this edifice (Appendix A). This big altered dome makes up nearly a third of the volume of the Eastern Edifice, but, as yet, no material appropriate for dating has been found. The pervasiveness of the hydrothermal alteration in both domes contrasts with the fresh younger lavas that make up the rest of the edifice, suggesting that the early episode of alteration had ceased prior to renewed construction of the edifice.

2.2. Stratified interval: ash bed, dacite breccia and sandy interlayers

Similarly altered and also along the lakeshore is a stratified sequence of breccia with an overlying ash bed (Fig. 4). Exposed along ~35 m of shoreline near the NE notch, these strata dip ~20° E—

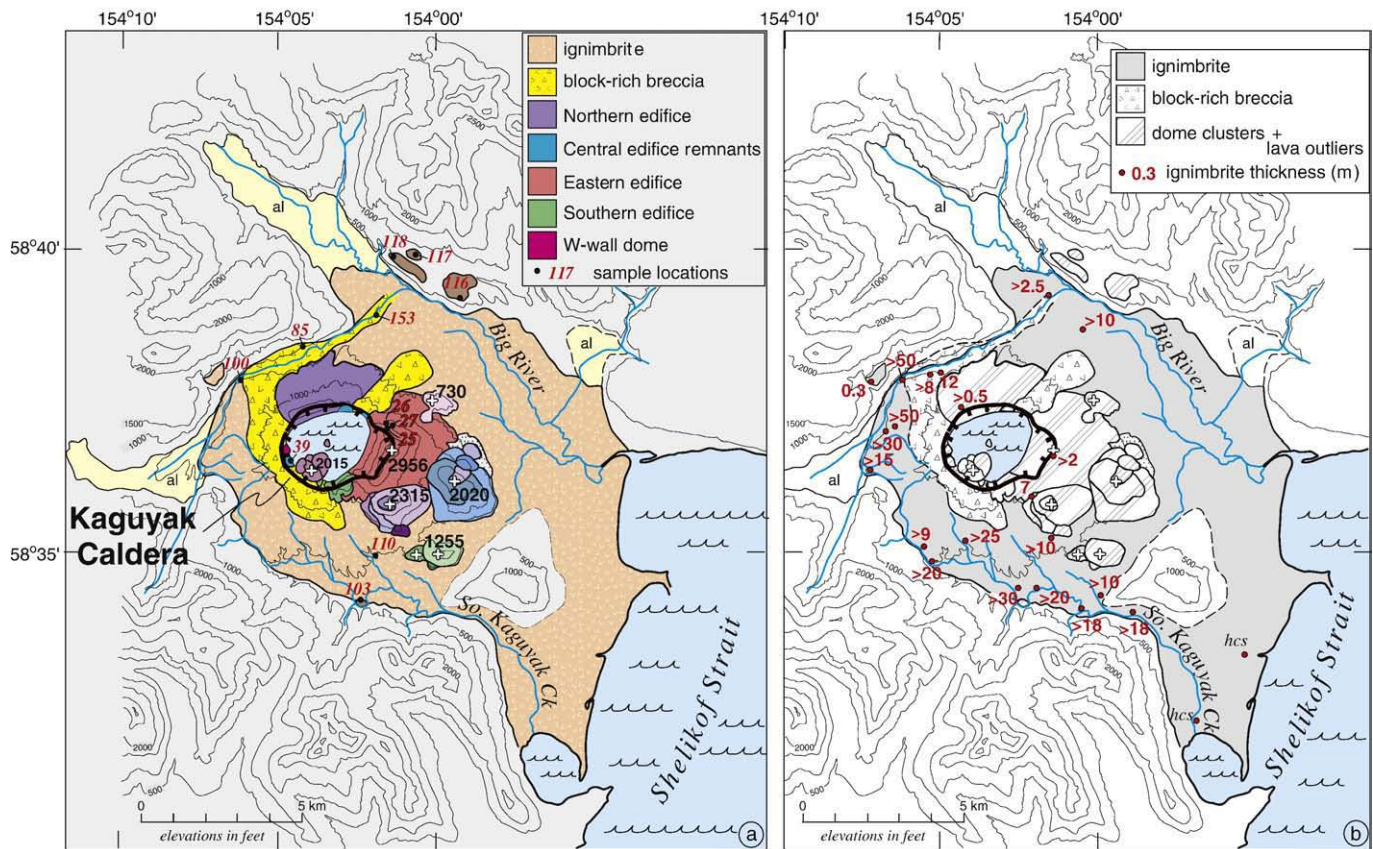


Fig. 3. (a) Schematic map of Kaguyak dome field. Only components of the dome field cut by caldera are in key. Elevations (in feet above sea level) marked by "+" are used to name extra- and intracaldera dome clusters. Unlabeled island in lake is the tip of another postcaldera dome. Lava outliers discussed in text are labeled by sample numbers 103, 110, 116, 117, and 118 (corresponding to Y-103, etc.); extent of remnants is colored brown. Patterned orange area shows probable original extent of ignimbrite; less is preserved and exposed now; ignimbrite emplacement dammed surrounding drainages and subsequent reworking created abundant pumiceous alluvium (al). Most of surrounding grey area is Mesozoic sedimentary basement (Riehle et al., 1994). Selected sample locations discussed in text are in red italics (e.g., 153). (b) Exposed ignimbrite thicknesses (in meters) are marked in red numbers; text describes the three sites that have an exposed base. Hyperconcentrated sand flows (hcs) make up a significant portion of exposures in the lowlands near the Kaguyak coastline and were part of the postignimbrite sedimentation (see Section 8.4).

outboard relative to the caldera wall. They are sandwiched between the old altered rhyodacite lava dome (of package 1) and a fresh grey lava lobe belonging to much younger package 2, with the dipping strata apparently draping the underlying rhyodacite dome. Although the lower contact of the stratified package is hidden by talus, its alteration places it close in time to the altered domes of package 1.

In the lower half of the exposure, the 10-m-thick breccia includes mostly dense angular to subrounded lava clasts from cm to decimeter-scale (a few as large as 1 m), with a minor amount of sandstone and mudstone clasts (some silicified) and laterally discontinuous intercalated 1–2-m-thick intervals of crystal sand up to several meters long. The lava clasts are plagioclase-rich and dacitic (65.6% SiO₂; Y-30b, Appendix A), compositionally and petrographically unlike either of the two (package 1) domes exposed in the wall (Fig. 6), and the deposit is most likely a remnant of a lava dome once positioned inboard of the caldera wall that syneruptively crumbled and shed clasts downhill.

The upper half of the stratified sequence is a 10-m-thick white to buff altered and Fe-stained massive lithic-rich ash bed with scattered small (<0.5-cm) crystal-poor lava clasts. These crystal-poor clasts suggest affinity of the tuff with the petrographically similar dacite dome of package 1 (exposed 700 m southward), with the tuff emplaced during an early explosive stage of dacite dome growth. The tuff drapes the flank of the rhyodacite dome, evidence that the latter is the older of the two domes. Thus, the earliest stage of the Eastern Edifice (package 1) was built by emplacement of (at least) three silicic lava domes: first, a rhyodacite dome (Y-31), followed by a crystal-rich dacite dome now represented only by

stratified breccia (Y-30b), and then by a voluminous crystal-poor dacite dome (Y-51, 52; Fig. 4).

2.3. Eruptive package 2: grey exogenous dome lobes/flows

The second eruptive package exposed in the caldera wall includes three closely related grey lava flows (or exogenous lobes of a truncated dome) which make up much of the northern part of the Eastern Edifice and are: (a) a basal flow, barely exposed through the thick scree that drapes nearly half the caldera wall here (sample Y-35); (b) a 300-m-thick middle flow (Y-24, 28, 29, 34) that directly overlies both the basal flow and the stratified clastic section just described; and (c) a 100-m-thick upper flow capping the ridge-nose that forms the east wall of the caldera (Y-23; Fig. 4). Each of the three flows is partly glassy and pervasively chunky to irregularly jointed. Only the upper flow has a distinct columnar glassy base where it rests sharply on the middle one.

All flows in this eruptive package are compositionally and petrographically similar (~65–67% SiO₂; Fig. 6, Appendix A), with the small plagioclase phenocrysts (15–20%) characteristic of the Eastern Edifice, two pyroxenes, no olivine, and nearly ubiquitous scattered microvesicular to sugary textured crystal clots (pl+cpx+opx) up to 1 cm across.

The middle flow yields a plagioclase ⁴⁰Ar/³⁹Ar age of 197 ± 58 ka (Y-28; Table 1), which lies nicely between the bracketing eruptive packages dated at ~300 and 60 ka. This fits reasonably with field evidence that there was likely a significant time gap between emplacement of packages 1 and 2 as expressed by: (a) the striking contrast between

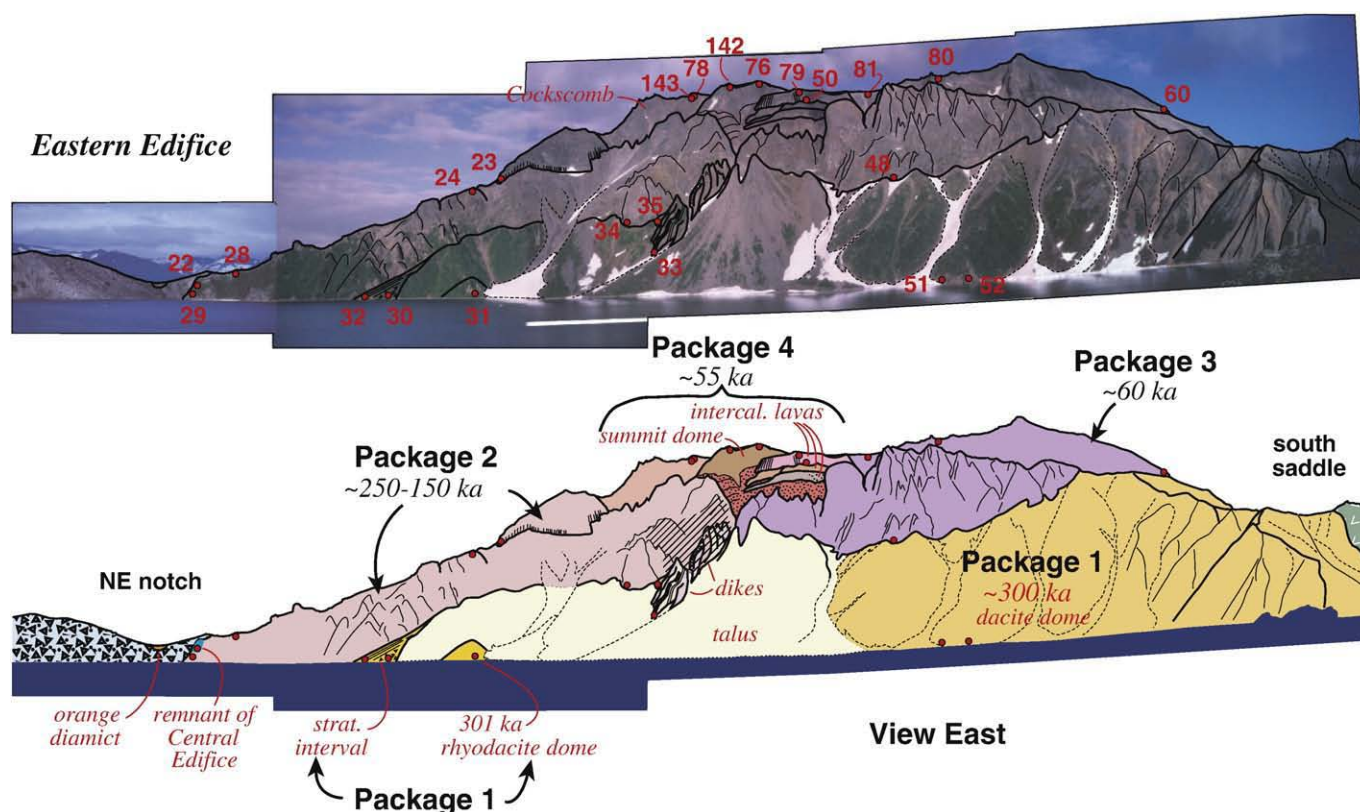


Fig. 4. Photo and sketch of Eastern Edifice exposed in SE wall of caldera. Sample locations numbered and marked with red dots. Four eruptive packages are each composite as described in text. For clarity of text discussion some units within packages are labeled on this figure: The stratified interval (strat. interval) in package 1 includes a dacite breccia and a thick lithic-rich ash bed; A dike complex within package 2 is surrounded by halo of alteration (hachured); A stack of stratified oxidized scoria falls (red and stippled) marks the base of package 4; Summit dome, intercalated lavas (intercal. lavas), and Cockscomb lava flow of package 4 are also labeled. Ages are based on $^{40}\text{Ar}/^{39}\text{Ar}$ dates in Table 1 by A. Calvert (USGS, Menlo Park). The northeast notch (NE notch) is the lowest point on the caldera rim, only ~30 m above lake level; it is filled by deposits of a block-rich breccia (“Big Breccia”) from the dome disruption-avalanche (blue, patterned) that preceded caldera collapse. In the saddle is a small patch of an orange fragmental deposit attributed to phreatic explosions related to emplacement of the post-caldera island dome (orange diamic). Just to its right is a small remnant of a banked-in lava (Y-22) that originated from a Central Edifice that was almost entirely destroyed during Holocene caldera collapse. Lava lobes from the Southern Edifice (grey-green, far right) overlap the much older, hydrothermally altered Eastern Edifice at the low point on the southern rim (south saddle).

the fresh glassy lava of eruptive package 2 and the pervasively altered lavas of underlying package 1; and (b) the concave morphology of the contact between older package 1 and younger package 3 (in the southern half of Eastern Edifice) that suggests the former suffered significant (glacial) erosion before emplacement of the latter. This contact, projected northward along the caldera wall and under the talus cover, argues similarly for erosion between emplacement packages 1 and 2 (Fig. 4).

2.4. Dike complex

At least 30 dikes, strongly defined by vertical joints, create “fins” trending N30°W with much of the altered host rock now eroded from between them, the dikes shedding a slabby talus apron just north of center of the Eastern Edifice (Figs. 4, 7). These mutually injecting dikes clearly cut through the oldest lava of package 2 and, slightly hydrothermally altered themselves, appear to have altered a large zone nearby in the middle lava, implying this 100-m-wide complex was the feeder system for the package 2 phase of this edifice. Vertically jointed dike segments, mostly grey to brown, are each 1–4 m thick, are partly glassy, and are cut by horizontal and inclined cross joints. Two of the dikes were analyzed and, at 66% SiO₂, both are compositionally similar to the more silicic portions of the eruptive package (Fig. 6).

They are petrographically similar to, though slightly finer-grained than, the units they intrude, both having small plagioclase and two pyroxenes (Appendix A). The intrusive relationships, synemplacement

alteration, petrography, and composition suggest that this dike complex was active over a period of time that included at least the oldest and middle lavas of emplacement package 2, and probably the upper lava, as well. Additionally, it seems likely that parts of this dike complex could also have been the feeder system for package 3 lavas described below.

2.5. Eruptive package 3

Eruptive package 3 includes two thick overlapping dacite lava flows that together make up the upper third of the southern part of the Eastern Edifice wall. Both are in direct contact with the older altered dacite dome of eruptive package 1, where the lower one overlies a concave erosional surface on the older dome (Fig. 4). This lower lava (~69% SiO₂; Fig. 6) is internally grey, although alteration on surfaces and joints make it appear slightly orange. Massive with vertical joints in the basal zone, it becomes more brecciated upward and makes up a spire-forming cliff on the SE caldera wall (Fig. 4).

The upper lava flow is as thick as ~100 m and forms the southern half of the Eastern Edifice summit ridge. Everywhere sampled, the lava is grey, glassy and commonly micropumiceous. The distinct columnar-jointed base at the southern tip and southeastern flank of the summit ridge is in striking contrast to the older, pervasively orange-altered dome of eruptive package 1 which it overlies. Compositionally homogeneous, four samples from different locations are all slightly less silicic (~67% SiO₂) than the lower lava,

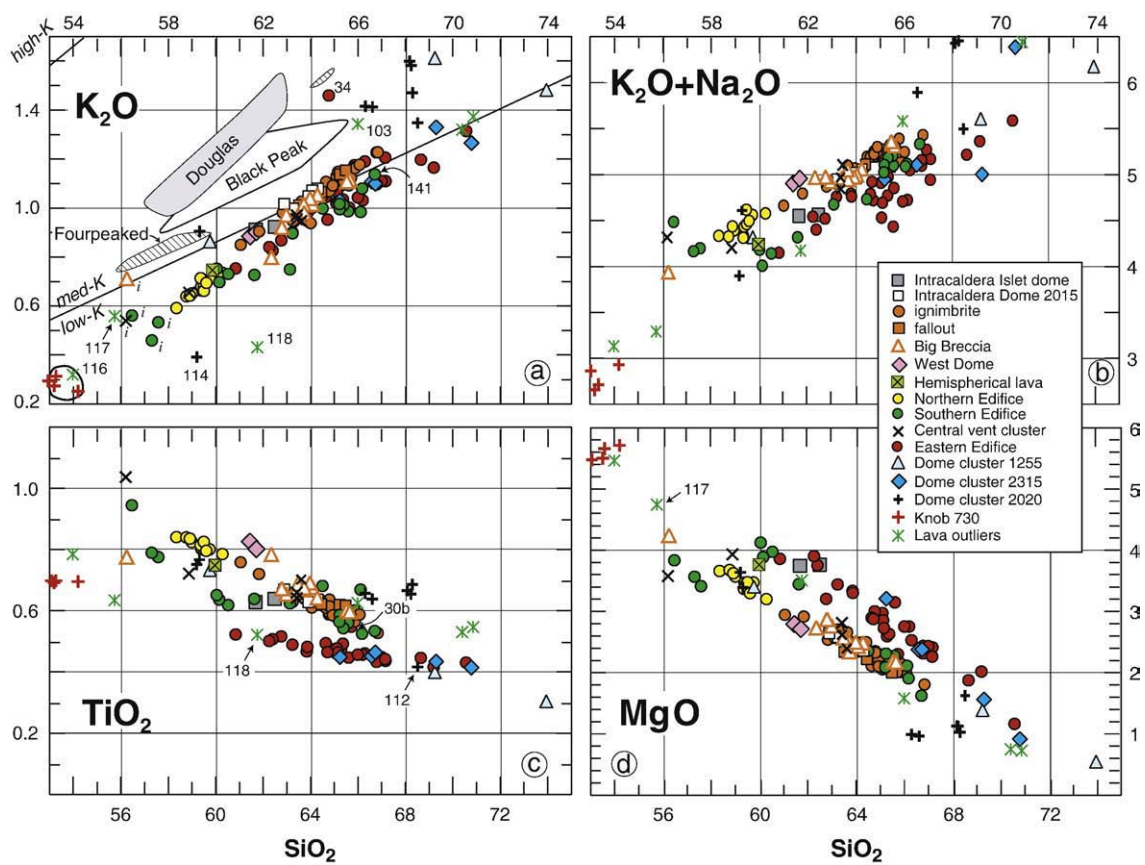


Fig. 5. Chemical plots of entire suite of Kaguyak dome field. Fields for Fourpeaked volcano, Mount Douglas (authors' unpublished data) and Black Peak (Adleman, 2005) are shown for comparison (see Section 13). Sample numbers are shown for select data discussed in text (117 is Y-117); sample locations in Figs. 3, 4, 10, and 19; (a) K₂O vs. SiO₂; High, medium, and low-K boundaries extended from Gill (1981); slight hydrothermal alteration of Y-114 and 118 results in K₂O-loss; Analyzed inclusions (i) in Southern Edifice lava unit and in Big Breccia clast labeled in this panel only; (b) Total alkalis vs. SiO₂; (c) TiO₂ vs. SiO₂; low TiO₂ characterizes Eastern Edifice lavas, as does low FeO and P₂O₅ (not shown), except for a breccia clast in package 1, Y-30b, discussed in Section 2; (d) MgO vs. SiO₂; higher MgO characterizes Eastern Edifice lavas, as does higher CaO (not shown). See Appendix C for all chemical data.

although both flows are similarly plagioclase-rich with few mafic phenocrysts, which are exclusively tiny ortho- and clinopyroxenes (Appendix A).

⁴⁰Ar/³⁹Ar dates yield 56 ± 4 ka for the lower flow (Y-48) and 65 ± 4 ka (Y-60) for the upper flow (Table 1), suggesting they were emplaced in close succession ~60 ka—more than 200 kyrs after emplacement of the package 1 dome on which they rest.

2.6. Eruptive package 4: summit sequence

Four units (61 to 65% SiO₂) make up the youngest part of the Eastern Edifice (Fig. 4): (a) stratified scoria intercalated with a stack of thin lavas capped by one thick lava; (b) a thick craggy lava here called the 'cockscomb'; (c) several outboard lavas; and (d) a blocky summit dome. These are similar petrographically in that all but two include olivine

Table 1
³⁹Ar/⁴⁰Ar and K/Ar dates

Sample	Unit	Separate	Age (ka)	% ³⁹ Ar released	K/Ca	Comment
³⁹Ar/⁴⁰Ar						
Y-15	Northern Edifice	gm	26.0 ± 5	71.9	0.182	Plateau age
Y-28	Eastern Edifice	pl	197 ± 58	70.3	0.024	Plateau age
Y-31	Eastern Edifice	pl	301 ± 65	69	0.023	Plateau age
Y-40	Big Breccia	gm	6 ± 5	98.6	0.273	Plateau age
Y-48	Eastern Edifice	gm	56 ± 4	49.1	0.673	Plateau age
Y-56	Southern Edifice	gm	29 ± 4	82.5	0.487	Plateau age
Y-60	Eastern Edifice	gm	65 ± 5	41.8	0.554	Isochron age
Y-90	Dome 2315	pl	125 ± 91	77	0.011	Plateau age
Y-108	Dome 1255	gm	173 ± 3	80.4	0.93	Plateau age
Y-116	outlier lava	gm	121 ± 12	63.2	0.059	Plateau age
Y-134	Southern Edifice	gm	42 ± 11	100	0.338	Isochron age
Y-142	Eastern Edifice	gm	92 ± 37	53	0.142	Plateau age
Y-147	Dome 2020	gm	259 ± 5	80.8	0.702	Isochron age
Y-151	Southern Edifice	gm	34 ± 8	100	0.508	Plateau age
K/Ar				% radiogenic	K₂O	
Y-54	Southern Edifice	Gm	28 ± 12	1.59	0.9415	

Notes: Separate refers to what was dated: groundmass (gm); plagioclase (pl). K/Ca ratios calculated from measured ³⁹Ar/³⁷Ar ratios. Analyses by A. Calvert, U.S. Geological Survey Geochronology laboratory, Menlo Park, CA. Analytical techniques similar to Calvert and Lanphere (2006).

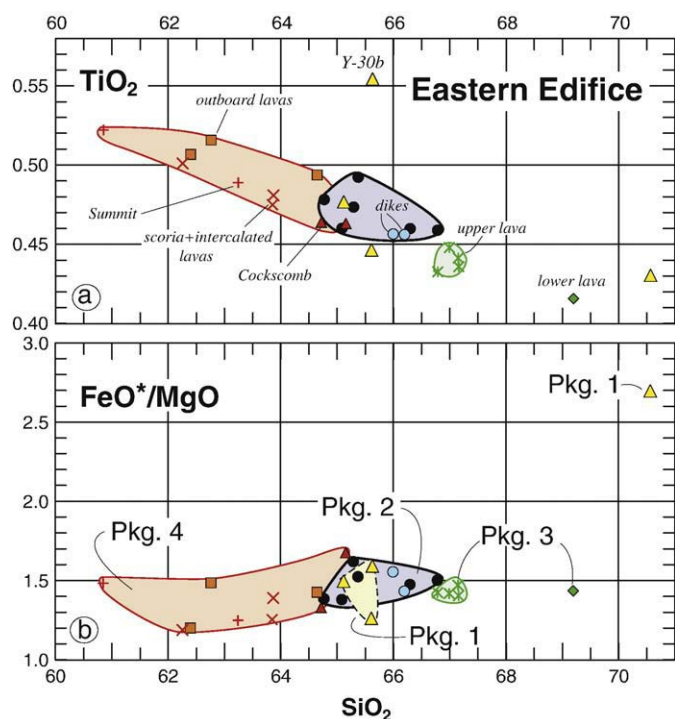


Fig. 6. Chemical plots of Eastern Edifice flows grouped into four eruptive packages (Pkgs. 1–4) as labeled in lower panel; select units within eruptive packages discussed in text are labeled in upper panel; Y-30b is a clast from the stratified sequence of Package 1. (a) SiO₂ vs. TiO₂; (b) SiO₂ vs. FeO*/MgO.

phenocrysts, which are virtually absent in other Eastern Edifice lavas. All erupted within a relatively short time, since the entire sequence is younger than package 3 flows (~60 ka), and the summit dome yields an age of 92 ± 37 ka (Y-142, Table 1). The overlapping ages indicate that eruptive package 4 was emplaced soon after underlying eruptive package 3.

2.6.1. Scoria and intercalated lavas

A stack of stratified oxidized scoria falls (red in Fig. 4) fills irregular topography on the underlying lavas of eruptive episodes 2 and 3 as

well as a funnel-shaped (probable vent) area below the summit dome. Three thin black lava flows are intercalated within the scoria section, which is overlain by another, thicker lava flow and by the blocky dome that makes up the true summit.

A block collected from one of the thin flows is one of the least silicic Eastern Edifice units (~62% SiO₂), but is one of the few units in package 4 without noticeable olivine. The 30-m-thick lava flow (~64% SiO₂) that caps the sequence of thinner lavas lies directly beneath the summit dome and forms part of the summit ridge to its south. In this flow, olivine phenocrysts join the typical (pl+cpx+opx) assemblage, which also includes scattered plagioclase phenocrysts as large as 5 mm (unusual for this Edifice) and scattered vesicular crystal-rich clots (cpx+opx±ol) as large as 1.5 cm across (Appendix A).

2.6.2. The cockscomb

Ragged spires along the narrow summit ridge at the NE end of the Eastern Edifice (Y-78, 143; Fig. 4) are part of a lava flow resting on the irregular surface of the middle flow of eruptive package 2 and banking against the uppermost unit of that same package; it dips outboard from the caldera wall ~30° SE, and is overlain by the summit dome (Fig. 4). This 30–40-m-thick pale-grey dacite lava (~64.5%–65% SiO₂; Fig. 6) is compositionally and petrographically similar to the thick lava at the top of the stratified scoria section described above, including the scattered large plagioclase and distinctively vesicular crystal clots (Appendix A). Their petrographic and chemical similarities and their equivalent mutual positions beneath the summit dome suggests their eruptive affinity; they may have been continuous prior to extrusion of the summit dome.

2.6.3. Blocky summit lava dome and outboard lavas

Summit Peak 2956 is a dome of dark blocky lava and the youngest eruptive unit of the Eastern Edifice. It is the least silicic (~61–63% SiO₂, Y-76, Y-142; Fig. 6) of the Eastern Edifice lavas and has small phenocrysts (pl+opx+cpx±trace ol) as is typical of this complex (Appendix A).

Another set of three glaciated lava flows (62.5%–64.5% SiO₂) on the north flank of the Eastern Edifice (nearly due north of the summit) dip outboard ~30–35° (Y-25, 26, 27; Fig. 3). All have small phenocrysts and include olivine (pl+ol+cpx+opx), which is conspicuously abundant and large (to 2 mm) in the upper two flows. Bathed in talus from the



Fig. 7. Photo of Eastern Edifice dike complex exposed in southeast wall of caldera; relief visible in dike set at left is ~30 m. Note 2-m-tall person in foreground bushes for scale.

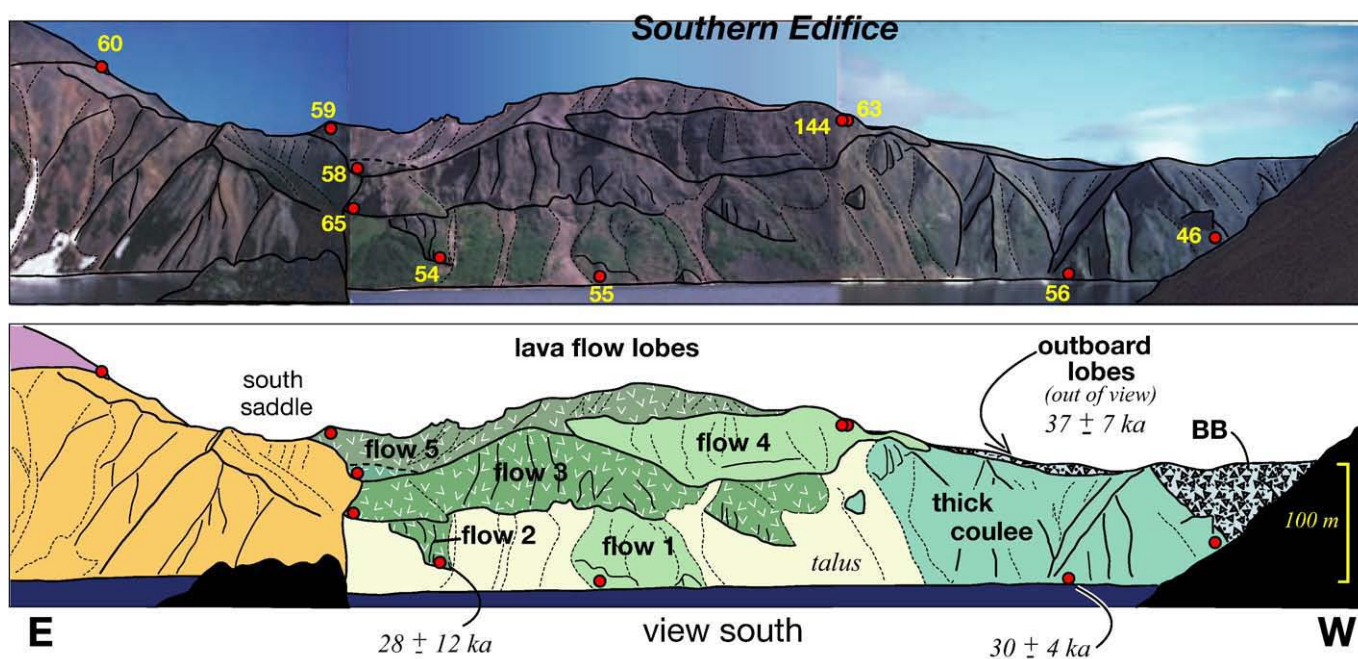


Fig. 8. Photo and sketch of Southern Edifice exposed along south wall of caldera. Sample locations marked with red dots, sample numbers in yellow. $^{40}\text{Ar}/^{39}\text{Ar}$ dates in Table 1 by A. Calvert (USGS, Menlo Park); Date on outboard lobes (just out of view beyond caldera wall) is an integrated age of two samples from the same unit (see Table 1). The outboard lobes and two thick coulees (only one shows in photo) are part of the same eruptive unit and are overlain by thinner lava flow lobes (greens). Lava flow lobes that originated from Southern Edifice vents inboard of the caldera wall bank against the much older altered Eastern Edifice lavas (orange in sketch, see Fig. 4) at the low point on the south rim (south saddle). Solid green lava flows 1 and 4 are less silicic (60–61.5% SiO_2) than patterned lava flows 2, 3, and 5 (63–66% SiO_2); petrographic distinctions discussed in Section 3. Big Breccia Holocene dome-collapse avalanche deposit (BB; discussed in Section 6) overlies the Southern Edifice.

thick lava ridge above (Y-23 of package 2), it is not clear whether these three flows are beneath that package 2 flow or are banked against it. Compositional similarities with the rest of package 4 flows, presence of olivine, and dissimilarity with the rest of the Eastern Edifice lavas, suggest that these outboard-dipping flows have affinity with eruptive package 4.

2.7. Summary of Eastern Edifice

Stratigraphy and dating thus suggest that the Eastern Edifice was built during at least four episodes (~300 ka, ~250–150 ka, and ~60 ka, the latter including two final episodes close in time that emplaced packages 3 and 4) with significant erosion only between the oldest eruptive episode (package 1) and the rest. Chemical and petrographic affinities link the episodes, suggesting that episodic growth of the Eastern edifice resulted from a common long-lived magma reservoir.

3. Southern Edifice

The Southern Edifice, as exposed in the southern caldera wall (Figs. 3, 8), consists of two thick lava coulees side-by-side (65–66% SiO_2) on its western end and five thinner interleaved massive to brecciated lava flows (60–66% SiO_2) on its eastern end. The interleaved flows are banked against and overlie the adjacent altered dome of the Eastern Edifice as well as one of the thick Southern Edifice coulees on the west, showing them to be the youngest components of the Southern Edifice. Outboard of the caldera wall are four glacially eroded, cliffy buttresses, each intricately jointed (hackly, chunky, with small local column sets) and locally sheared into thick subunits of flow breccia. Compositionally similar to lavas on the inner caldera wall, with no apparent breaks between wall and outboard, each buttress appears to consist of a single lava flow that protrudes outward as a flat-topped shoulder which dips slightly southward, away from the caldera.

Far smaller than the adjacent Eastern Edifice, the Southern Edifice has a more restricted range of SiO_2 (60–66%, Fig. 9) and its products are generally richer in phenocrysts (20–40%), with abundant plagioclase commonly 4 mm and as big as 8 mm. The mafic phenocryst assemblage is dominantly hornblende + orthopyroxene ± magnetite in all units, with some small, sparse olivine in a few units and, rarely, clinopyroxene microphenocrysts. The thick, older flows contain hornblende and orthopyroxene prisms generally larger (commonly 5 mm and up to 8 mm) than in the overlying lava flows. This contrasts starkly with the small phenocrysts, two-pyroxene ± olivine mafic assemblage and absence of hornblende in the Eastern Edifice (Appendix A).

3.1. Thick coulees

The western limit of the Southern Edifice ends in a cove formed by encroachment of post-caldera Dome 2015 on the truncated southern caldera wall (Figs. 2 and 3). Exposed on this wall are what appear to be two thick glassy lava flow lobes, both of which reach from the lakeshore nearly to the rim (at least 100 m). One of these coulees, adjacent to the stack of flows that makes up the eastern half of the Southern Edifice (described below), is thickly columnar to chunky jointed (with horizontal joints interrupting vertical ones). The other, in the cove corner (out of view in Fig. 8), makes a steep cliffy promontory and is very blocky with irregularly jointed faces that shed coarse blocky talus. Both are overlain by the Holocene “Big Breccia” unit (described in Section 6), which fills a funnel-shaped gap between the two and obscures any contact between them. Both lobes are thick enough that they could be two domes extruded right near the present caldera wall. We think, however, that these are coulees from a vent slightly inboard, since both lobes are lithologically and compositionally nearly identical to one another and are very similar to two of the lava buttresses that form stubby shoulders on the outboard southern slope of the caldera (Fig. 3). All are compositionally homogeneous

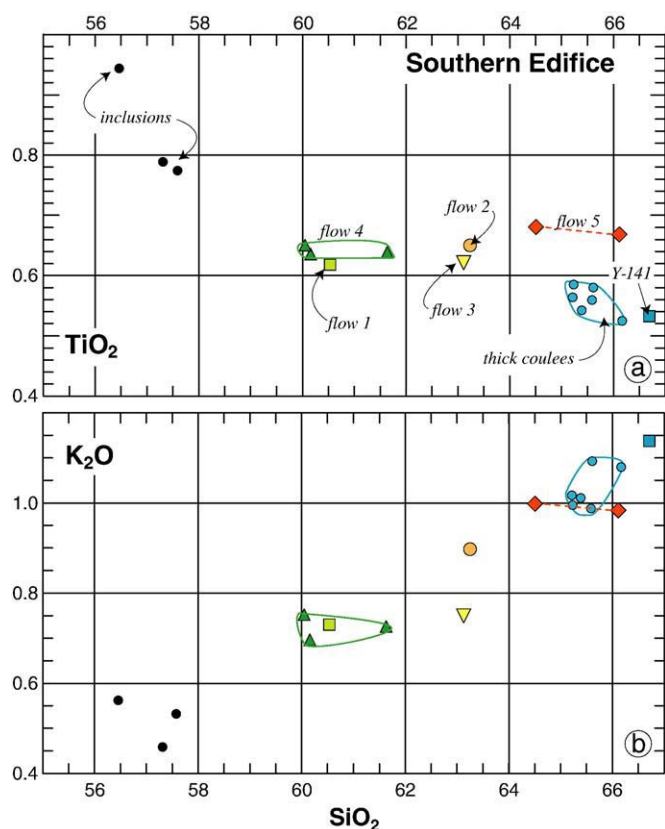


Fig. 9. Chemical plots of Southern Edifice flows; a) SiO_2 vs. TiO_2 ; b) SiO_2 vs. K_2O . Individual units labeled in upper panel are the same in the lower. Thick coulees are the oldest components; Y-141 is a Southern Edifice lava (probably related to the thick coulees) that flowed across the caldera and is only exposed in the north wall (see Fig. 10). Flows 1–5 are lobes that originated from vents located within the present caldera. Analyzed inclusions are all fine-grained mafic blobs found in the thick coulees.

(~65–66% SiO_2 ; Fig. 9) and very crystal-rich (as much as 40–45% phenocrysts) with many large plagioclase (to 7 mm). All have subequal amounts of hornblende and orthopyroxene, with clinopyroxene sometimes present as scarce microphenocrysts, but no olivine (Appendix A). Abundance of conspicuous slender elongate mafic prisms (1–2% up to 7 mm in length), which include both hornblende and orthopyroxene, distinguishes these mineralogically from the adjacent stack of interleaved brecciated lava flows (described below; Section 3.3) that have few, if any, of these large prisms.

These two coulees are the oldest part of the Southern Edifice, with younger portions of the complex banked against and overlapping the more eastern of the two (Fig. 8). Three $^{40}\text{Ar}/^{39}\text{Ar}$ dates yield similar results: one sample from one of the coulees collected in the caldera wall at lake level yields 30 ± 4 ka (Y-56), and two dates from one of the coulees on its outboard flank are within 2σ error and yield a weighted mean of 37 ± 7 ka (Y-134, 151; Table 1, Fig. 8).

3.2. Southern Edifice flow remnant on northern wall

An additional component of the Southern Edifice is a 10-m-thick lava flow exposed 2 km away across the present-day lake and intercalated with Northern Edifice lavas high on the north caldera wall (Y-141; Fig. 10). So striking are the abundant large mafic minerals (~3%) and many conspicuous large (to 8 mm) slender mafic prisms and large plagioclase phenocrysts (35–40%), that this one thin flow stands out strongly in lithologic contrast from those above and below it. At 67% SiO_2 (Fig. 9), it is compositionally unlike any other Northern Edifice lava (discussed in Section 4; Figs. 5, 11; Appendix A), but is much like Southern Edifice lavas; it is clearly a remnant of another lava flow originating from the Southern Edifice. Perched at ~1500 ft elevation on the NNE shoulder of today's truncated north rim, this lava flow must have been extruded from a Southern Edifice vent at least that high, which was destroyed by caldera formation. We suggest that this flow, petrographically and compositionally so similar to the thick coulees discussed above (Section 3.1; Fig. 9), erupted not long after they did, from the same (or overlapping) vent.

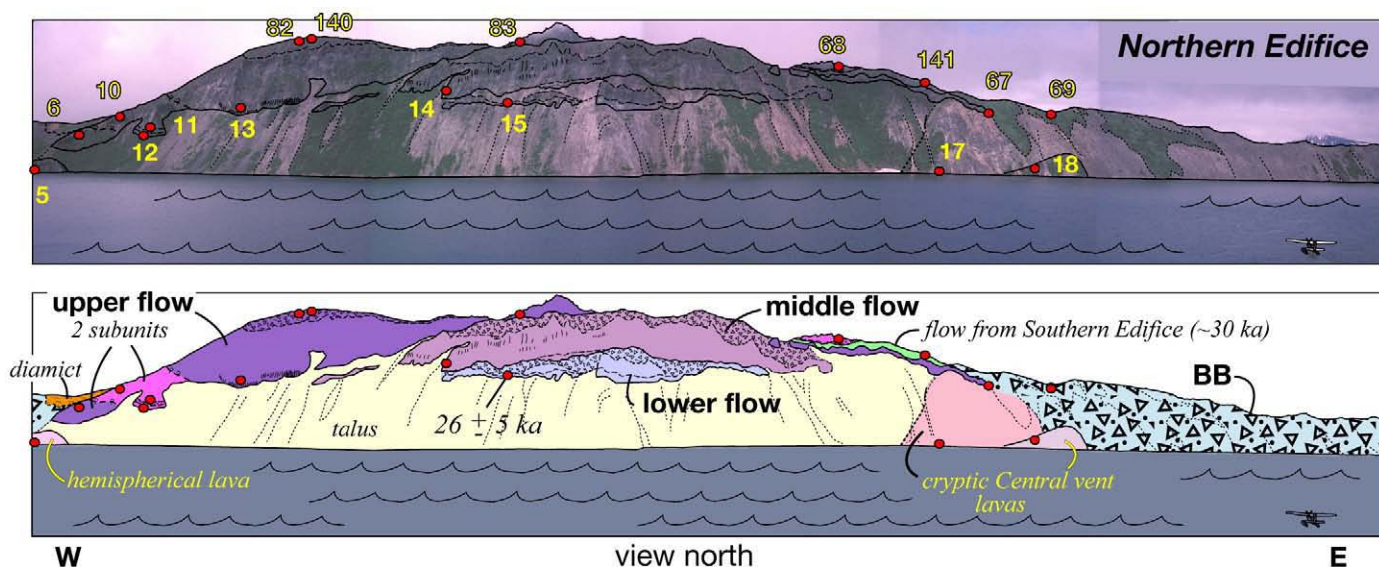


Fig. 10. Photo and sketch of Northern Edifice exposed in northern wall of caldera, view is ~2.5 km across. Float plane (lower right) for scale in lake. Sample locations marked with red dots; sample numbers in yellow. Three thick flows make up most of the edifice, the lowermost mostly buried by talus (pale yellow); the upper flow includes two subunits; brecciated tops are patterned and pronounced jointing shown schematically. Y-141 is the only remnant of a flow that originated from the Southern Edifice vents and is compositionally unlike the rest of the flows exposed on the northern wall; it is sandwiched between the two subunits of the upper Northern Edifice flow. Two older domes of the cryptic Central vent cluster (Y-17, 18 at the far right of the edifice) are overlain by thin lobes of Northern Edifice flows. The Big Breccia unit (BB; patterned) laps onto the eastern shoulder of the Northern Edifice. It filled in what was once a large gap between the Northern and Eastern Edifices. One $^{40}\text{Ar}/^{39}\text{Ar}$ date from the lowest flow shows the entire Northern Edifice is ≤ 30 ka; the intercalated Y-141 is also ~30 ka.

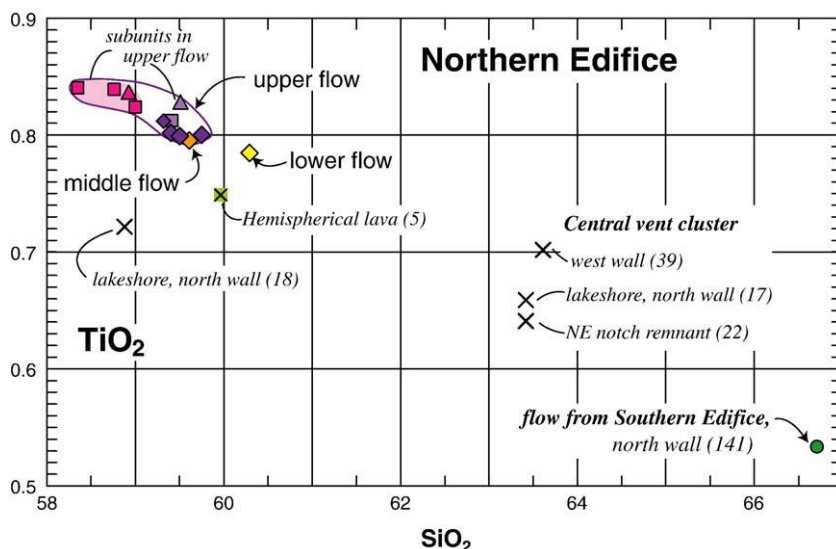


Fig. 11. TiO₂ vs. SiO₂ for lava flows exposed in the North wall of the caldera, including products from the Northern Edifice, Southern Edifice, and cryptic Central Vent cluster. Northern Edifice flows include three thick flows (lower, middle, and upper). In the outlined field for the upper flow are symbols showing the subunits within it, including two thin lavas that flowed west (squares) and east (triangles) of the edifice summit, and one thick flow that makes up the Northern Edifice summit; light purple symbols are from the thin basal subunit; pink symbols from the second thin subunit; dark purple symbols from the thick unit. Compositionally and lithologically distinct sample Y-141 is a lava flow from the Southern Edifice intercalated between the Northern Edifice flows. The hemispherical lava (sample Y-5) probably vented inboard of the caldera and banked against the older Northern Edifice. Remnants of the cryptic Central Vent cluster (X's) exposed on the north and west walls of the caldera are compositionally distinct from Northern Edifice lavas. Sample numbers in parentheses (e.g., 18, 5). Refer to Fig. 10 for locations.

3.3. Interleaved massive and brecciated flows

Five lava flow lobes make up the eastern half of the Southern Edifice exposed in the caldera wall. No obvious erosional contacts or sharp flow boundaries separate them, but they are clearly distinct lobes as seen from a distance and sketched (labeled 1–5) in Fig. 8. The lavas can be characterized into two distinct types (Fig. 9): (a) Flows 1, 4, and one of the outer wall buttresses are more massive, less silicic (60–61.5% SiO₂), and have no large slender mafic phenocrysts but do include a small amount of olivine as microphenocrysts, in contrast with (b) Flows 2, 3, and 5, which are pervasively brecciated, more silicic (63–66% SiO₂), and have at least some large, long mafic phenocrysts (up to 1%) and no olivine (Appendix A). Thus, these are two mineralogically and chemically distinct flow types that erupted within a short period of time.

All of the flows—even the more massive ones—are brecciated to some degree, with only a minor amount of coarse, somewhat indurated matrix between coherent angular clasts up to 2 m across. Most of the breccia and the intricate jointing of the more massive zones is chaotic. There is, however, locally developed layering in the breccia, seen best in flow 3, that dips outboard ~20°S, implying an inboard vent over what is now the caldera lake. Absence of sharp contacts or erosion surfaces between any flows in the stack suggests little time between their emplacements. Indeed, it seems most likely that these flows, and the stubby flow buttresses on the outboard wall, originated from two compositionally and mineralogically distinct but contiguous vents that once occupied a spot not far inboard of the truncated wall; they erupted nearly synchronously and built the more easterly portion of the Southern Edifice. Flows 3–5 are certainly younger than the coulees that made up the western end of the Southern Edifice, since flow 3 banks against and flow 4 overlaps the massive coulee to the west. Flow 2 (Y-54) yields a K/Ar age of 28 ± 12 ka, suggesting that the entire flow stack was emplaced ~30 ka.

3.4. Summary of Southern Edifice

The Southern Edifice was mostly destroyed during Holocene caldera collapse, with lava flows and thick coulee remnants on

the truncated walls representing what was once a coalescence of at least four vents, all of which clustered inboard of the present caldera wall. With no evidence for erosion between any of the units exposed in the southern wall, not much time could have elapsed between their emplacements. ⁴⁰Ar/³⁹Ar and K/Ar dating suggest the same. Overlapping ages suggest that the entire Southern Edifice was relatively short-lived and emplaced ~30 ka.

4. North Wall: Northern Edifice and cryptic Central Vent cluster

Products of three different vents are represented on the north wall of Kaguyak caldera, between the low points along the rim from the NW to the NE corners. Most of the wall is made up of three thick flows that dominate the truncated Northern Edifice (Fig. 10). Secondly, at the eastern end, are intact remnants of two lavas from what is here called the “cryptic Central Vent”—a vent cluster that was once located within the area of the present lake and was almost entirely destroyed during Holocene caldera collapse. Thirdly, are two small remnants of lava flows important for their constraints on emplacement timing of three edifices: One is the thin lava flow that originated from the Southern Edifice and is intercalated with Northern Edifice lavas on the NE rim (Y-141, discussed in Section 3.2); the other is a hemispherical-shaped remnant in the NW corner (Y-5) which vented just inboard of the present caldera wall and is one of the youngest eruptive units of the pre-Holocene sequence (Fig. 10).

4.1. Northern Edifice

The Northern Edifice includes some of the least silicic of all lavas sampled in the Kaguyak region and a more restricted SiO₂ range (58–60% SiO₂) than either the Southern or Eastern Edifices (Fig. 5). This edifice is largely a pile of three thick overlapping lava flows—the upper two each as much as 90 m thick with oxidized, brecciated tops. Only the top 30 m of the lowest flow is exposed; it is probably much thicker but is buried by the thick talus that covers nearly half the northern wall (Fig. 10).

Both the lower and middle flows have gently domical upper surfaces with fairly symmetric distributions in cross section as exposed

on the truncated wall. This aspect, as well as the steep (only slightly modified) northern flank of the edifice shows these were sticky flows that did not travel far and suggests the vent(s) for both were centered virtually beneath them. The upper flow, however, clearly drapes the older part of the edifice unevenly, with the thickest accumulation (~90 m) overlying and banked against the western flank, but with only 10 m banked against the eastern shoulder. The highest part of the middle flow was never covered by the upper lava. This distribution requires that the upper flow must have bifurcated around a pre-existing high (built of the preceding lower and middle flows), thereby creating a west and an east lobe of the upper one. Thus, the vent for the upper lava must have been further inboard to permit this geometry.

All three of the thick flows typically have ~15% phenocrysts and are characterized by blocky to subequant plagioclase and ~1–2% mafics including hornblende and orthopyroxene (Appendix A). Hornblende seen in thin section is almost always relict (poorly preserved and largely resorbed), clinopyroxene is seen only as scarce microphenocrysts, and no olivine has been found. These mafics tend to be small (1–3 mm), in contrast to the 7–8 mm phenocrysts so common in the thick Southern Edifice coulees. Only in the lowest of these three flows are there some widely scattered large hornblende and orthopyroxene. However, scattered embayed and rounded quartz grains are seen (in thin section) in all of them.

4.1.1. Subunits

Compositional and lithologic differences between the three thick Northern Edifice lavas are small. Compositionally, the lowest flow is the most silicic (~60% SiO₂) and the only one to have some long slender mafic phenocrysts (to 7 mm), while the thick middle flow and most of the upper flow are slightly less silicic (~59.5% SiO₂; Fig. 11). Only the upper flow can be further divided into two thin basal and one thick upper units. The lowest thin unit at the base of the section is nearly identical lithologically and chemically to the thick upper portion. The second thin unit, however, is consistently less silicic (58.4–59% SiO₂) and has fewer total phenocrysts (10–12%) than either the underlying basal unit or the overlying thick upper one (Fig. 11). Although field evidence for separating these units is subtle in the west lobe—expressed only as a breccia zone between the two basal units and an intermittent columnar zone at the base of the upper thick section—it is striking in the eastern lobe. There, on the NE shoulder of the Northern Edifice, these two thin units are separated by a third thin flow—the silicic one (Y-141; 67% SiO₂) with abundant large slender mafic phenocrysts that originated from the Southern Edifice complex as discussed in Section 3.2. This intercalation of Southern and Northern Edifice lavas indicates that (1) there was some amount of time (however short) between emplacement of different parts of the Northern Edifice summit sequence, and (2) there was at least partial overlap in eruptive activity between the two complexes. This is corroborated by the one good ⁴⁰Ar/³⁹Ar date we have on the Northern Edifice, which is from the lowest exposure of the thick lower flow of the main edifice; it yields 26.0 ± 5 ka (Table 1). This implies that most of the pile was constructed in a relatively short time, since inception of the Northern Edifice was ~30 ka and the thin Southern Edifice flow intercalated within the summit sequence is also ~30 ka.

4.2. Cryptic Central Vent cluster

Two lavas exposed at the east end of the northern wall (Fig. 10) in the NE corner of the caldera are the largest remnants of what we infer to have been a moderate size vent cluster where the lake is now. Two additional remnants, nearly identical lithologically and chemically to one of these lavas, are exposed on opposite sides of the caldera (W and E). One of the remnants that forms a small ledge near the low NE notch is banked against the Eastern Edifice (Fig. 4), and another small remnant makes up part of the west wall of the caldera (Fig. 3). Positions of the

four remnants around the caldera require that the vent must have been somewhat central (i.e., a Central Vent). Furthermore, because the thickest preserved exposure is in the northeast corner, it also seems likely that this was once a sizeable dome, or set of flow lobes—large enough to extend thickly to the northeast corner. Although much of the vent cluster was destroyed during subsequent Holocene events (thus, 'cryptic'), some significant portion of its north-wall remnant must be talus-covered, obscuring the seemingly required relation of the oldest of the Northern Edifice flows (~30 ka) banked against the even older Central Vent complex (Fig. 10), which is also older than the Southern Edifice.

4.2.1. Lava flow remnants: northeast, east, and west

The two truncated lavas exposed at the east end of the north caldera wall span the compositional range of the cryptic Central Vent cluster (59–63.5% SiO₂). The smaller one (~59% SiO₂) forms a cliff rising 10 to 20 m up from the lakeshore (sample Y-18; Fig. 10). Although andesitic like the nearby younger Northern Edifice lavas exposed higher on the wall, this lava is compositionally different in having slightly higher MgO and lower TiO₂ (Fig. 11), and is lithologically different in having generally fewer phenocrysts (~10% total) and smaller mafics (1–2 mm). Overlapping this small lava remnant is a larger one ~100 m thick rising from the lakeshore nearly to the caldera rim, where it is overlain by flows of the Northern Edifice summit sequence (Y-67, Y-68) and by the 30 ka-lava flow from the Southern Edifice (Y-141). Massive and silicic (63.5% SiO₂) with prominent subvertical flow banding along the lakeshore cliff, this lava has more phenocrysts (15–20%: pl ≫ opx + trace hb + trace cpx) than the underlying lava, with distinctively subequant plagioclase (as large as 4 mm), and 2–3% mafics (typically 1–3 mm), including rare (but present) long slender mafic prisms (to 5 mm; Appendix A). In spite of compositional differences, only a shear zone with an apparent dip of ~20°W separates the two domes; there is no erosional surface or sharp contact between them. Thus, although they are chemically different (Fig. 11), they were apparently emplaced in close succession, and we consider both to be part of the cryptic Central Vent phase.

Two other lava remnants compositionally and lithologically nearly identical to the thick (63.5% SiO₂) lava described above are exposed in the caldera walls. The first is a small lava ledge ~500 m further clockwise around the wall, ~15 m above the lakeshore, on the opposite side of the NE notch (Y-22; Fig. 4). Although in outcrop this lava remnant might be mistaken for part of the Eastern Edifice, it is compositionally distinct from the lower TiO₂, higher MgO, and small-plagioclase lavas of the Eastern Edifice units (Fig. 5). With Eastern Edifice-type lavas above and below, this remnant ledge must be banked against the older lavas here (Figs. 3, 4).

A second lava remnant (63.5% SiO₂; Y-39, Fig. 3) forms a prominent cliffy point on the opposite side of the lake where the west wall begins to define a cove adjacent to intracaldera Holocene Dome 2015. Slender columnar joints incline variably along the shoreline for more than a hundred meters, and the outcrop extends more than half-way up to the rim (≥45 m), where it is overlain by the Holocene breccia deposit (described later). These three lava exposures on the NE, E, and W sides of the caldera—compositionally and lithologically so similar to one another (Y-17, 22, 39; Figs. 5, 11, Appendix A), and dissimilar to other nearby lavas—suggest that they were derived from the same vent.

4.2.2. Summary of cryptic Central Vent

A moderate-sized cluster of two to three vents beneath the present-day lake was largely destroyed during Holocene caldera collapse, but distribution of four lava remnants clearly show they erupted from a location that was either central or somewhat northeast of center of today's caldera. Although the cryptic vent lavas are not dated directly, ⁴⁰Ar/³⁹Ar ages on overlying Northern and Southern Edifice units provide an upper age limit of 30 kyr on the cryptic Central Vent cluster. This cluster must have predated the Southern Edifice on geomorphic grounds, also, since the Southern Edifice (Y-141) lava

perched at 1500' on the northern caldera wall requires that the space between the Southern and Northern Edifices had to have been filled by a lava pile at least that high (to permit the Y-141 lava to flow downhill). We suggest the Central Edifice predated inception of the Southern Edifice, filling the middle part of what is now the present caldera. Once the first phase (thick coulees) of the Southern Edifice was extruded, it blocked the second eruptive phase (Y-141 lava) from traveling southward; the lava flowed NNE instead, over the top of the Central Dome, and toward the NE shoulder of the Northern Edifice.

4.3. Hemispherical lava

Along the shoreline in the NW corner of the caldera is a small hemisphere-shaped lava outcrop enveloped by talus at one end and the Holocene breccia deposit (that makes up most of the west rim) at the other (Fig. 10). The lava (~60% SiO₂; sample Y-5; Appendix A) has a 6-m-thick, dark grey to brick red vesicular top that stands out as a prominent arched rim and emphasizes the overall hemisphere shape. Truncated by Holocene caldera collapse, this is a remnant of a (very) small dome or a lava flow lobe, exposed in near-perfect cross section. Lithologically similar to some of the thick flows of the North Edifice—although a little more crystal-rich than most (20–25% phenocrysts)—this lava has ~1.5% mafics, including at least a few long slender mafic phenocrysts (5 to 8 mm), and common subequant to blocky plagioclase (Appendix A). It is characterized by abundant pale-grey sugary-textured blobs (fine-grained mafic enclaves) that dot the outcrop and are as much as 10 cm across (commonly 1–4 cm). Compositionally somewhat different from Northern Edifice flows (lower Al₂O₃, TiO₂ and Na₂O, and higher MgO), and from Southern Edifice flows (higher TiO₂, lower Al₂O₃; Fig. 5), this is another separate lava erupted inboard of the caldera wall and banked against the oldest portion of the Northern Edifice.

5. West Dome

Only two lava outcrops peek out along the lakeshore from beneath the Holocene breccia deposit that makes up most of the west caldera rim (Fig. 3). One, the more southerly, is a lava remnant from the cryptic Central vent cluster described above. The more northerly, however, is less silicic (61.5% SiO₂), and is a remnant of another small extrusion, here

called the West Dome. The outcrop is only 100 m long, ~20–25 m high, and makes a small point that protrudes into the lake. Enveloped by the younger breccia at either end of the outcrop, most of it is partly glassy and coarsely chunky to hackly jointed. Slender inclined columns at the northern end of the outcrop (Fig. 12) show this to be the margin of a small dome that most likely banked against or intruded into ice as it was extruded (Lescinsky and Sisson, 1998). Somewhat less phenocryst-rich (~20%) than the thick coulees of the Southern Edifice, the West Dome has slightly smaller plagioclase, fewer total mafics (opx+trace hb), and less hornblende (Appendix A).

Although only subtly different lithologically from Southern Edifice flows, this dome is compositionally unlike all the other edifices exposed around the caldera walls and plots separately from them with respect to most major elements (Fig. 5; SiO₂, TiO₂, MgO, CaO). Lack of exposed contacts with other units provides few constraints as to relative ages. However, we suspect that it—like the Southern and Northern Edifices—postdates the building of the Eastern dome complex (so is younger than ~60 ka) because: (1) it is compositionally more like the products from the younger Northern and Southern Edifices than those from the older Eastern Edifice; (2) it erupted closer to the vents of the former; and (3) because the rock is fresh and not altered like the oldest components of the Eastern Edifice.

6. Big Breccia

A generally unstratified, coarse, grey fragmental deposit forms a Holocene apron distributed west and northeast around Kaguyak caldera (Fig. 3). As shown in photo/sketch Figs. 4, 8, and 10, the deposit thinly laps onto margins of the Eastern, Southern, and Northern Edifices. Both the northeast and west caldera walls are constructed of this diamicton; there would be no caldera lake if the deposit were not there. It fills what were low saddles between existing edifices, filling what were apparent drainages (WNW and NE) between the precaldra dome clusters. There is no evidence that this breccia ever covered the peaks or outer flanks of either the Northern or Eastern Edifices, and no evidence that it traveled far from source. Only when funneled into the Big River did it go farther than ~3 km. Three radiocarbon dates (locations along Big River marked with red Xs on Fig. 16)—two on organic soil from two locations on top of the breccia and one on charred twigs found in the deposit—yield essentially



Fig. 12. Thinly columnar-jointed lava at the margin of the Western Dome is evidence for synemplacement ice contact. Hammer is 32 cm long.

identical results: respectively, 6010 ± 100 ; 6010 ± 110 , and 6010 ± 160 ^{14}C yrs B.P. (Fierstein 2007). In agreement, a $^{40}\text{Ar}/^{39}\text{Ar}$ date for a lava block within the breccia yields 6.4 ± 5.0 ka (Table 1).

Similar in all exposures around the caldera, the grey-brown, gritty matrix includes almost no clay and is seriate with the rest of the deposit, which includes angular to subangular lava blocks, commonly up to 4 m and as big as 8 m. All blocks are largely glassy, fresh to oxidized (none hydrothermally altered), dense to micropumiceous lava; there is no pumice in this deposit. Young and unglaciated, the breccia apron is cut radially by V-shaped gullies that project skyward at the caldera rim (Fig. 13), indicating that the gullies were beheaded by caldera collapse and thus predate it.

This massive deposit, so strikingly unstratified in the caldera walls (even where >60 m thick), filled the headwaters of Big River to the northwest and was channeled clockwise (downstream) around the pre-existing Northern Edifice. Thick vegetation and mantling by the subsequent ignimbrite leaves the breccia deposit only patchily exposed along the banks of the river, where no stratification is seen in the deposit for the first ~ 7 km along its flow path (as far as Y-85 on Fig. 3). There, exposed in an eroded alcove on the left bank of Big River, the breccia is at least 25 m thick and is exposed for ~ 100 m upslope where it ran up the hillslope and banked against the Jurassic sedimentary basement. In this clast-rich exposure, most of the dense lava blocks are angular (some subrounded) and, although not as large as those in the caldera wall, many are still >1 m across. Only ~ 2.5 km farther downstream on the right bank is a long terrace exposure where the only stratification found anywhere in the deposit is expressed as a few graded flow units each 5–15 m thick. There (location Y-153 on Fig. 3), thick coarse zones with blocks to 2–4 m grade up into 2–4-m-thick zones in which only decimeter-sized blocks are the coarsest clasts. The clasts (subangular to subrounded) reside in a subordinate, coarse sandy matrix that is slightly indurated by widespread rusty-brown Fe-staining. Unlike any other exposure, the dominant grey lava clasts at this location (Y-153) are joined by a lesser population of clasts of similar lithology, but with white to Fe-stained rinds thick enough that they were likely acid-alteration rinds prior to outflow. Atop this deposit are ~ 8 m of post-breccia, stratified fluvial cobble-boulder gravel, overlain in turn by ~ 12 –15 m of stratified sand and gravel—all river deposits that

accumulated before Big River succeeded in re-incising through the thick breccia.

6.1. Clast types in breccia

All lava clasts in this breccia deposit are crystal-rich dacites (pl+cpx+opx+minor hb), some with as much as 30–40% phenocrysts, and others with as little as 12–15% (Appendix A). Plagioclase dominates the phenocryst assemblage in all, and in most clasts is blocky or subequant and large (to 4 mm). Mafics in most are conspicuous (0.5–3%, from 1–3 mm), and include at least some elongate slender prisms (opx and hb; 4–8 mm). A smaller fraction of the clasts have small plagioclase (i.e., Y-111) and more hornblende (i.e., Y-85; Appendix A).

Compositionally, the clasts fall into four groups. The dominant clast type has 63–64% SiO_2 and shows similarities in major-element data with both the Central Vent lavas and some of the Southern Edifice lavas (labeled “1” in Fig. 14a). Trace-element data (slightly higher Zr, Ba, and Nb contents relative to the Southern Edifice lavas) suggest that this set of clasts have more magmatic affinity with the older Central Vent cluster (Fig. 14b; only Zr shown). The second set is more silicic (65.5% SiO_2) and is similar to the thick coulees of the Southern Edifice. The third group, with $\sim 62\%$ SiO_2 (represented by sample Y-111) has fewer total phenocrysts (15–18%) and fewer total mafics ($<1\%$) than most and is lithologically and compositionally similar to the West Dome lava (Y-36, 38; Appendix A, Fig. 14). The rare fourth clast type is a finely vesicular microdiorite that looks like and is compositionally similar to inclusions in nearby Southern Edifice lavas. We conclude that these differences in chemistry and lithologies reflect clast contributions from several flows and/or domes. Notably absent from the clast suite analyzed are any similar to banked-in flow Y-5, Southern Edifice flows 1 and 4, and any Northern Edifice or Eastern Edifice flows.

6.2. Dome disruption: Big Breccia event

The following considerations require that the Big Breccia deposit was emplaced catastrophically during a single explosive disruption episode of a dome or dome complex that was once located west-of-



Fig. 13. Beheaded gullies cut in the Big Breccia deposit along the NE notch of the caldera rim; unstratified even though >60 m thick (continues below view). View northwestward from N toe of Eastern Edifice (crag in foreground). Big River gorge (in shadows) is beyond the sloping gullied breccia deposit; vegetated far wall of the gorge consists largely of stratified Jurassic Naknek Formation (marine sediments, Riehle et al., 1994).

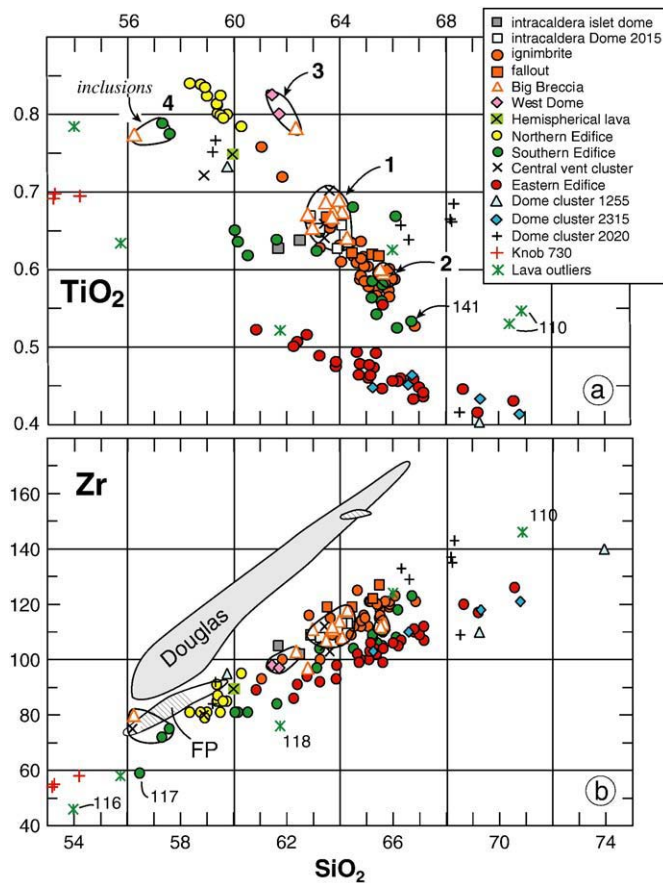


Fig. 14. (a) TiO_2 vs. SiO_2 shows that clast types in the Big Breccia are in four groups—those that are chemically like the Central vent cluster (1), those like the thick coulees of the Southern Edifice (2), those like the Western Dome (3), and those like inclusions found in the Southern Edifice thick coulees and Central vent lava (4). Sample Y-141 (filled green circle, 141) is the lava flow from the Southern Edifice preserved as a remnant on the northern wall, sandwiched between Northern Edifice lavas and discussed in Section 3.2. (b) Zr vs. SiO_2 shows that clast types can be distinguished by trace-element data, as well. Note that Zr values for breccia clasts in group 1 are slightly higher than those of the Southern Edifice, and suggests affinity with the Central vent cluster. Ba and Nb (not plotted) show similar relationships. Fields for nearby Mount Douglas and Fourpeaked Volcano (FP) shown for comparison.

center, between the Northern, Eastern, and Southern Edifices, within the area of the current caldera lake:

- 1) The thick, unstratified deposits and lack of internal erosional unconformities suggest a single emplacement episode, not a piecemeal accumulation of flow units.
- 2) Radial distribution of the deposit (NE, WNW, and SW) requires a central source within the area occupied by the subsequent caldera.
- 3) Compositions of most of the clasts in the breccia suggest that their main source was either a dome related to the pre-existing (and somewhat overlapping) Southern Edifice and Central vent complexes (both of which had source vents in the position of the current caldera lake), or (as we prefer) a compositionally slightly different dome (here called the Southwest Dome) that extruded on top of them.
- 4) Subordinate clast contributions to the breccia include some that are compositionally similar to the West Dome, the older cryptic Central Vent cluster, and the Southern Edifice. Analyzed clasts clearly do not include the compositionally distinctive Northern or Eastern Edifices, or the banked-in Y-5 lobe or Southern Edifice flows 1+4. Thus, the dome must have been positioned such that disruption included minor contributions from the former several, but not from the latter.

- 5) The main fraction of analyzed clasts are essentially identical—both in major and trace element chemistry—to analyses of postcaldera intracaldera Dome 2015 (Figs. 5, 14).

Considering list 1–4 above, and considering that an established conduit is commonly reused by subsequent eruptions (e.g., Mount St. Helens, Lipman and Mullineau, 1981), we infer that the Big Breccia deposit resulted from catastrophic disruption and collapse of what was probably a new dome extruding close to the position of present-day Dome 2015.

7. Precaldera topography: inferences from deposit distributions

The preceding descriptions paint a picture contrary to previous suppositions (Wood and Kienle, 1990; Riehle et al., 1996) by clearly showing that precaldera Kaguyak was never just a single stratovolcano. Rather, it was a focus for dome-building with at least 4 dome complexes and several additional domes centered within or exposed around the walls of the present caldera. Fig. 15 shows the dome-building sequence over time. These include three large dome complexes still largely present around the rim of the caldera (Northern, Eastern, and Southern Edifices), one small dome exposed in the west wall (West Dome), mere remnants of a once-large Central Vent complex, and what was the youngest precaldera dome (Southwest Dome) preserved only as the Big Breccia deposit distributed around the present caldera rim (Fig. 16). Each of the larger dome complexes is multi-component, built by several successive viscous flows that piled on top of or next to each other. Only the Eastern Edifice represents a very long eruptive time span (>200,000 years). As described above (Section 6.2), thick accumulations of the Big Breccia deposit forming the NE and WNW walls of the caldera filled what had been radial drainages between edifices, providing a sense of the topographic relief that existed prior to emplacement of the Big Breccia and subsequent caldera collapse (Fig. 16a). Several other deposit distributions provide evidence for precaldera topography and constrain vent positions and relative dome sizes and ages for some of the edifices:

- 1) On stratigraphic grounds, the cryptic Central Vent cluster was older than the Northern Edifice (see Section 4: North Wall: Northern Edifice and cryptic Central Vents and Fig. 10). The three compositionally similar remnants of this effusive vent now exposed on the northern, western, and northeastern caldera walls suggest that three flows originated centrally and flowed in different directions (Fig. 15d). Had the Central vent been simply a large ovoid-shaped edifice, a significant amount of erosion would have been required to create a gap between the lava remnants we now see on either side of the NE notch; this seems unlikely. Rather, emplacement as flow lobes would preserve (even help create) the gap between the lava remnants on either side of the NE notch (Y-17 on the north wall, Fig. 10 and Y-22 on the east wall, Fig. 4). In this scenario, it seems required, too, that these flow lobes bifurcated around the older dome exposed beneath Y-17 on the north wall, only the very edge of which is preserved as ledge Y-18 (Figs. 10, 15d). This bifurcation preserved the gap between the Northern and Eastern Edifices—filled later by the thick Holocene Big Breccia deposit. Similarly, the lava remnant on the west wall is engulfed by the breccia deposit, also suggesting this was a relatively small flow lobe rather than part of a single massive ovoid dome.
- 2) The vent(s) for the Northern Edifice flows were clearly inboard of the present caldera wall, but were separate enough from the Central Edifice conduit system that their compositions are distinctly less silicic (Figs. 5, 15e, f). Whereas the two lower thick flows of the Northern Edifice are fairly symmetrical in cross

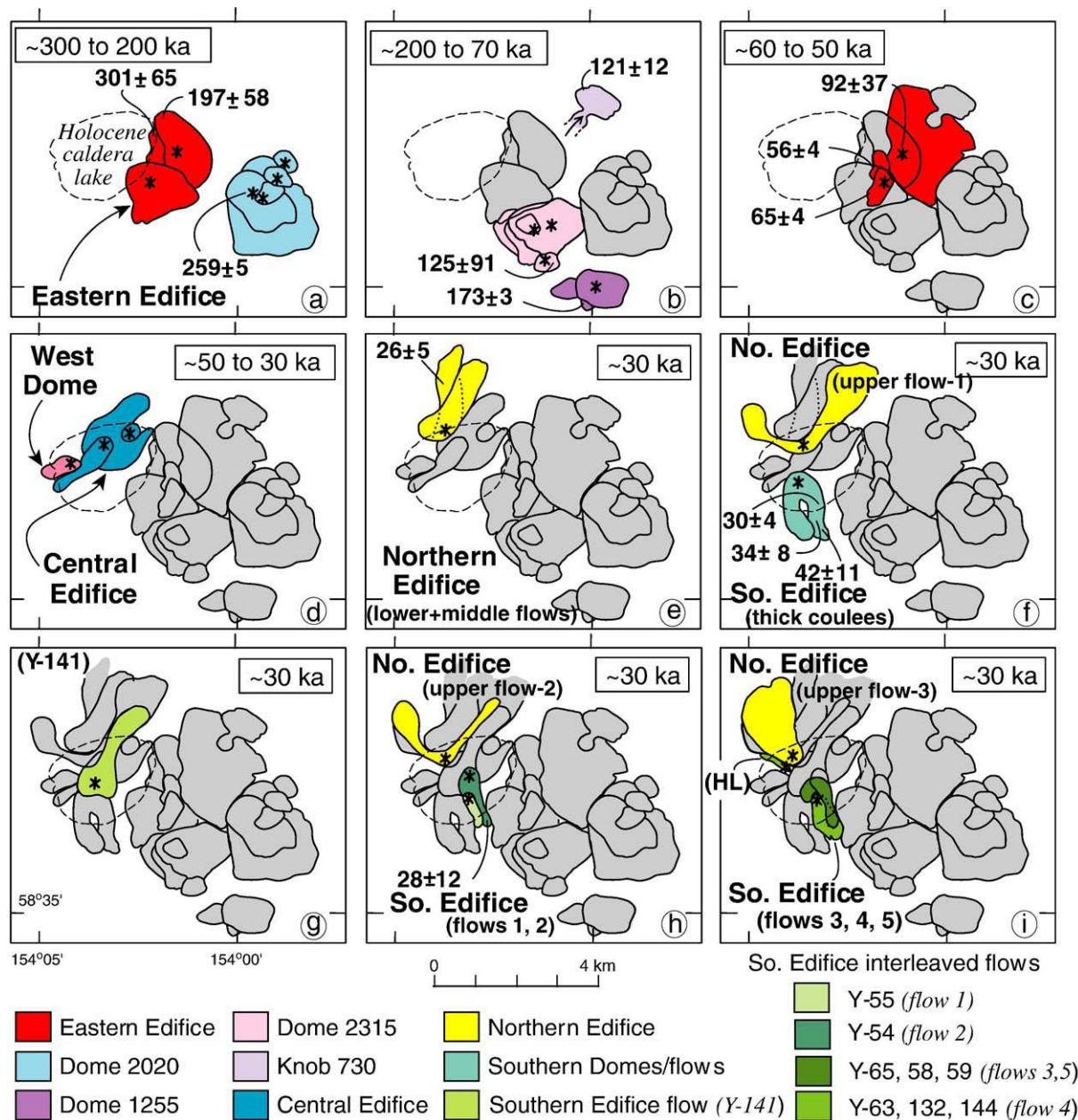


Fig. 15. Kaguyak dome-field building sequence from ~300 ka to ~30 ka. Each unit is colored (as in Key) when first erupted, then is colored grey in subsequent panels. Asterisks mark vents not obscured by overlapping lava flows. Holocene caldera lake (dashed) shown for reference. Northern Edifice (No. Edifice) lower and middle flows predated inception of the Southern Edifice (panel e). The Northern Edifice upper flow and the Southern Edifice are approximately coeval. Southern Edifice flow Y-141 (panel g), is intercalated between two thin subunits of the Northern Edifice upper flow (upper flows-1 and 2, panels f and h). The remainder of the upper Northern Edifice flow (upper flow-3, panel i) forms a thick summit cap. Five interleaved lava flows from Southern Edifice vents are stratigraphically numbered 1–5 (panels h and i). The Hemispherical lava (HL, panel i) is another separate lava erupted inboard of the caldera and banked against the oldest portion of the Northern Edifice. The scale is the same in all panels.

section, the upper summit sequence (two thinner subunits beneath a thick upper flow) is not (Fig. 10). The distribution of the summit flows requires a vent that distributed most of its products northward. The moderate swell of the pile of previous Northern Edifice flows (i.e., thick lower and middle units) must have provided enough relief to bifurcate the two lower subunits of the subsequent summit sequence (Figs. 15e–i). Thus, these two subunits are preserved thinly on the east shoulder of the Northern Edifice, with most of the volume having flowed toward the western shoulder.

3) The thin middle lava flow (Y-141; Fig. 10)—shown to have affinity with the thick coulees of the Southern Edifice—is po-

sitioned high (1500' elevation) on the Northern Edifice east shoulder. This requires the vent for that flow lobe to have been at least at that elevation. It also requires a downhill flow path that would permit the lava to flow from the Southern Edifice vents to the Northern Edifice shoulder. Thus, no significant drainage could have separated these vents from the Northern Edifice. Instead, it seems required that the Southern Edifice vents were perched atop of or at least overlapped an older lava pile (Fig. 15g). The most likely older lava is the cryptic Central vent cluster, now mostly destroyed, but represented by several remnants including the one exposed beneath the thin flows in the northern wall (sample Y-17, Fig. 10).

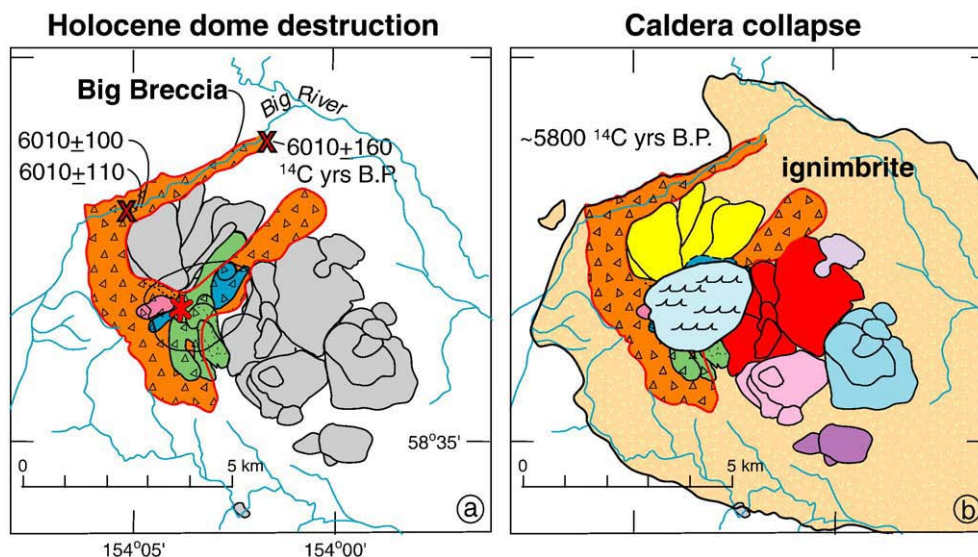


Fig. 16. (a) Holocene events at Kaguyak began with another lava dome extrusion (red asterisk) on top of the pre-existing pile of lavas from the Central Edifice, Western Dome, and Southern Edifice. Catastrophic dome disruption shed a thick, unstratified diamicton (Big Breccia) radially around the vent. Red "X"s along Big River mark locations of ^{14}C -dated soil and twig samples. (b) Caldera collapse ~ 200 years later truncated the Northern and Eastern Edifices, the West Dome, and the Southern Edifice; it largely destroyed the Central Edifice, leaving only small remnants preserved on the caldera wall (Fig. 10). All units colored as in Fig. 15.

- 4) While the Central Vent cluster filled relief such that it permitted a lava to flow from the Southern to the Northern Edifice (Fig. 15g), it could not have extended too far westward since (a) the summit sequence of Northern Edifice flows thickens westward and evidently filled a low spot (Figs. 15f, h), and (b) we think it likely that the hemispherical outcrop at the west end of the Northern Edifice is a banked-in flow lobe (Y-5; Fig. 10) from a vent just west of the main Central Vent (Fig. 15i; see Section 4).

8. Caldera-forming eruption

The plinian or subplinian eruption that led to collapse of the central portion of the Kaguyak dome field distributed a proximal pumice-lapilli fall and inundated the surrounding area with a modest sized ignimbrite. A fine-grained coignimbrite ash elutriated during ignimbrite emplacement is widespread to the southwest—typically 3–5 cm thick as far as 80 km WSW. The ash has been widely correlated by its distinctive low- TiO_2 oxide minerals and low- K_2O glass compositions determined by electron microprobe (Fierstein, 2007). The ash layer is also well dated at ~ 5800 ^{14}C yrs B.P. (Fierstein, 2007), which shows that the caldera-forming event postdated destruction of the Southwest Dome and emplacement of the Big Breccia by only ~ 200 years (see Section 6 about Big Breccia).

8.1. Fallout

8.1.1. (Sub)plinian

Near-vent coarse lapilli fall (63.5 to 65.5% SiO_2) has been found in only seven proximal locations, all within 3 to 4 km of the caldera rim (Fig. 17c). At three of these locations where the deposits are best preserved—two to the NW (Y-126, 136) and one to the SSE (Y-131, Figs. 17c, Appendix B)—the fallout clearly underlies the ignimbrite. Thickest (>80 cm, base not exposed) SE of the center of the caldera (atop Dome 2315), the fallout is as much as 45 cm thick to the SW but only 3–9 cm thick to the W and NW. The coarsest clasts are found where the deposits are thickest, with pumice clasts as big as 9.5 cm found E of the caldera center (atop Dome 2020, Figs. 3, 17), 7 to 6.5 cm to the W and SW, but no larger than 3 cm to

the NW. Only two locations of more medial plinian fallout have been found; one, a (slightly disturbed) granule layer 8 to 10 cm thick in the headwaters of the Savonoski River ~ 22 km WSW of the caldera (location K-2673A), and another a 2 to 3 cm normally graded fine to very fine ashfall atop a lava bench near Snowy Mountain ~ 45 km SW of the caldera (location K-2681A, Fig. 17). We have done little work very far NE of Kaguyak, and thus far—although we have looked for it—have found no Kaguyak fallout as far as 7 km north or ~ 15 km east of vent. Beyond that distance, however, others have reported ash layers that might be correlative with Kaguyak fallout, as discussed below (Section 8.1.3; Kaguyak ash correlatives).

Fallout pumice lapilli are white, buff, or grey and include sparse banded (white and grey) pumice. Lapilli textures range from evenly vesicular to more coarsely, irregularly vesicular clasts. The latter invariably contain conspicuous dark blebs, which are commonly elongate crystal clots (as big as 1.5 cm in length and as thin as ~ 1 mm) consisting of 1-mm pyroxenes and fewer plagioclase crystals. The clots were clearly stretched syneruptively and are commonly surrounded by large vesicles, apparently having focused vesicle nucleation. No stratigraphic significance within the fallout has been determined for these different textural varieties, and even the more finely vesicular clasts can include a few clots. Although in three locations the more finely vesicular, clot-poor clasts predominate, the two textural types coexist in all locations.

Preservation of coarse fallout at only a few sites so close to vent seems odd for a plinian deposit, even in Alaska where erosion is typically rapid and vigorous, and suggests the possibility that there may never have been a widespread plinian fall, but rather only localized near-vent accumulations of fallout from pumice showers attending low fountaining that fed directly into ignimbrite outflow. That the initial explosion disrupted the pre-existing dome field is evident in the fall deposits, for they are everywhere rich in fresh, grey, glassy crystal-rich dacitic lava lithic clasts derived from dome lavas. A minor fraction of the lithics are hydrothermally altered yellow and orange, a few (not all) of them fine grained and crystal poor. These are most likely from the oldest part of the Eastern Edifice—the only strongly hydrothermally altered and crystal-poor rocks exposed in the caldera walls. An even sparser component is sedimentary lithics derived from the Jurassic basement, implying there was little explosive reaming of the vent under the caldera.

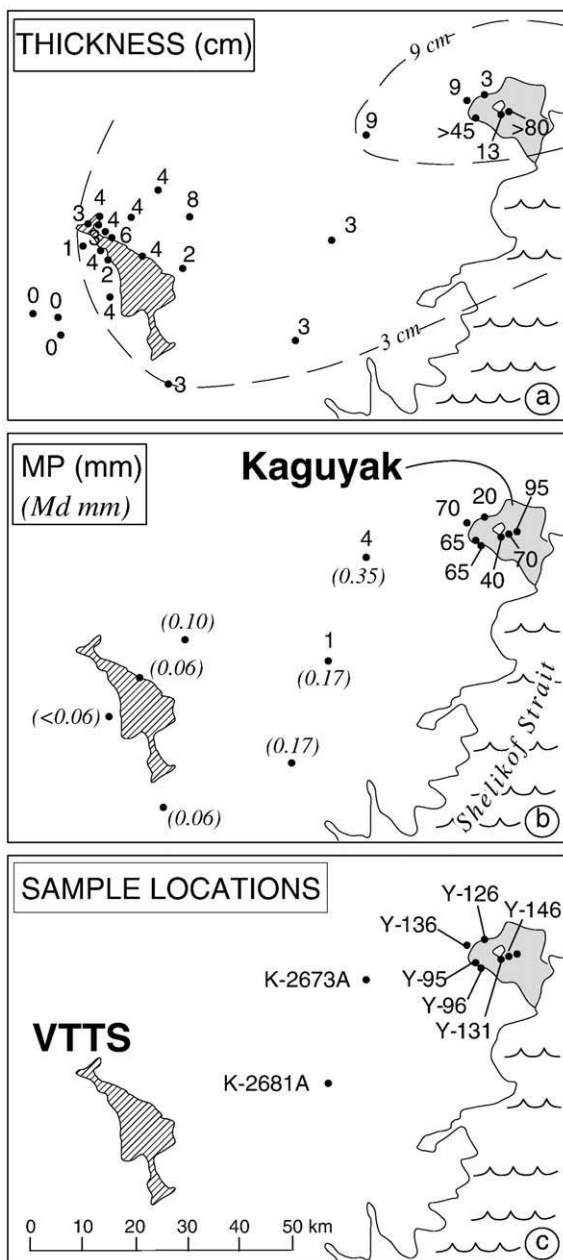


Fig. 17. Characteristics of Kaguyak fallout, both proximal pumice fall and more distal coignimbrite ashfall: (a) Thickness of fallout (cm), see Fig. 1 for 1.5-cm isopach; (b) Maximum pumice-clast size (MP) and median grain size (Md) in fallout (in mm); (c) sample locations mentioned in text. Original extent of Kaguyak ignimbrite is shaded light grey; Valley of Ten Thousand Smokes ignimbrite (VTTs) shown by diagonal lines.

8.1.2. Coignimbrite ash

Coignimbrite ash elutriated during Kaguyak ignimbrite emplacement was distributed regionally—far more widely than the lapilli fall (Fig. 1)—and is so distinctively bright orange and fine grained that it serves as a marker tephra in the Valley of Ten Thousand Smokes/Katmai area as far as 80 km to the southwest (Fierstein, 2007). Syneruptive oxidation of fine ignimbrite ash particles is not uncommon, a similar phenomenon that allowed Fierstein and Hildreth (1992) to recognize salmon-colored fine coignimbrite ash interstitial to coerupted (white) plinian fall lapilli in some of the Novarupta 1912 deposits (their Layer B₁). Distribution of the Kaguyak coignimbrite ash is well documented up to 80 km SW of vent in and near the Valley of Ten Thousand Smokes where it is very fine grained (Md < 0.06 mm). It is also tentatively correlated with a 2-cm-thick ash

layer near Brooks Camp, 100 km west of vent, but has not been found still farther west (Fig. 1 and Fierstein, 2007). There is, apparently, some mixing of (sub)plinian fallout with the Kaguyak coignimbrite ash within 45 km of the caldera in the southwestern sector, as reflected in both thickness and grainsize. Median deposit grainsize 22 km SW of vent is 0.35 mm, but decreases to 0.10 mm 40 km farther (Fierstein, 2007). Because we cannot be sure of the fraction of coignimbrite and fine plinian contributions, thickness and grain size values in Fig. 17 include total deposit characteristics at each location.

8.1.3. Kaguyak ash correlatives

Our own data do not extend far NE of Kaguyak. However, we think that ash layer 1B of Reger et al. (1996) on the Kenai Peninsula and Pinney's (1993) Y-ash near the Valley of Ten Thousand Smokes, which they correlate with it, are both Kaguyak ashfall. Microprobe analyses of glass shards published by Reger et al. (1996), Pinney (1993), and Fierstein (2007) are permissive of this correlation (Fig. 18). Stratigraphic correlations in the Valley of Ten Thousand Smokes (Fierstein, 2007) confirm that Pinney's (orange-colored and very fine) Y-ash is the Kaguyak coignimbrite ash. Confident in this correlation, we include their locations on Fig. 1, showing Kaguyak ash as thick as 2 cm on the Kenai Peninsula (~280 km NE). Riehle et al. (1999) also described a 2-cm-thick "pink" ash layer we tentatively correlate with the Kaguyak ash on Afognak Island ESE of Kaguyak, as well as a 20-cm-thick lapilli layer ~15 km E of Kaguyak and a 5-cm-thick fine grey ash layer ~40 km N of Kaguyak. In all the cases cited, the authors were unsure of the source of the ash units they described, and in all cases microprobe analyses of glass shards are permissive of correlation with the Kaguyak ash (Fig. 18). We are aware of only one other volcano along the Alaska Peninsula arc that has such high silica and low K₂O glass contents—Augustine volcano (Fig. 18). Unfortunately, glass data alone are insufficient to distinguish between Augustine and Kaguyak ashes (FeTi oxide data, potentially more definitive (Fierstein, 2007), are not published for Augustine). However, the stratigraphic agreement between Pinney (1993) and Fierstein (2007), similarity in mineral assemblages (two pyroxenes and a little hornblende), color (in most cases), and glass analyses lead us to include those locations in approximating the extent of the Kaguyak ash and in drawing thickness isopachs used to calculate volumes. Nowak (1968), too, described a

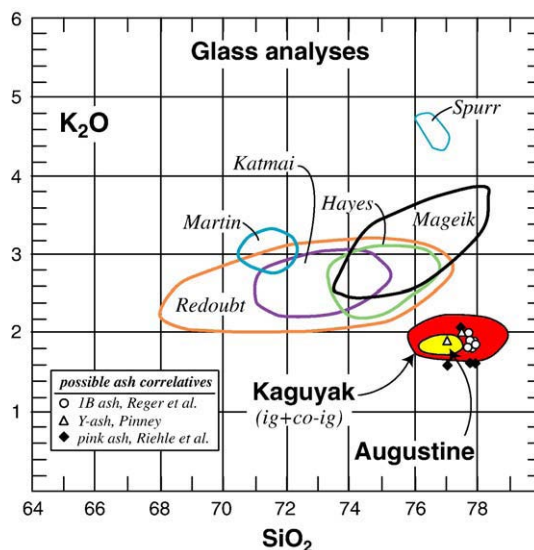


Fig. 18. Microprobe analyses of glass shards and pumice from Aleutian arc volcanoes near Kaguyak. Data for Redoubt, Hayes, Spurr from Riehle (1985); for Augustine from Riehle (1985) and Johnston (1978); data from Katmai, Martin, Mageik, and Kaguyak from Fierstein (2007). Ash layer 1B of Reger et al. (1996) on the Kenai Peninsula, Y-ash of Pinney (1993) in the Valley of Ten Thousand Smokes, and "pink ash" of Riehle et al. (1999) are all possible correlatives with the coignimbrite ash from Kaguyak.

3.5-cm fine pale yellow ash with minor hornblende (reported as ~5500 yrs B.P.) along the Kukak Bay coastline. Although no microprobe analyses are available, we include the sample location as probable Kaguyak ash on Fig. 1 as well.

8.2. Ignimbrite

The Kaguyak ignimbrite is typically tan to salmon-colored, unconsolidated to barely sintered, and moderately homogeneous with no obvious systematic compositional zoning. Many exposures show several pumice and/or lithic concentration zones (PCZ, LCZ; typically 0.25 to 2 m thick) in the upper half—evidence for internal flow units or shearing—although no systematic compositional differences have been found. Although the ignimbrite must have initially filled the surrounding lowlands as far as the seacoast (a straight 13 km line from the center of the caldera—longer along a flow path), the deposit is now heavily vegetated and either eroded or widely concealed by alluvial deposits along the Big River and South Kaguyak Creek drainages (Fig. 3). Local incision shows the primary ignimbrite to be >50 m thick where it filled the pre-existing Big River gorge NE of the caldera, as much as 12 m thick nearby but above the gorge rim on the north flank of the Northern Edifice, >30 m thick where it filled South Kaguyak Creek ~4 km south of the caldera, and still >18 m thick another 4 km downstream toward the coast (Fig. 3).

The ignimbrite was deposited on the irregular topography of the caldera rim, but only a few patches remain or are exposed, including 2 m atop the Eastern Edifice summit. Much of it might have been eroded, but it seems likely that lack of widespread ignimbrite deposits on or near the caldera rim is in part due to emplacement processes that minimized accumulation on the proximal high ground in favor of the surrounding valleys (Similar lack of near-vent pyroclastic flow deposition is noted by Scott et al., 1996 for the 1991 climactic eruption of Pinatubo.). In very few places is the base of the ignimbrite exposed, so the full thickness of the deposit is almost never seen. The three exceptions are: (1) an ignimbrite veneer thinning to 30 cm (and overlying poorly preserved lapilli fall) perched on a flat mesa ~4 km NW of the center of the caldera and nearly 300 m above present-day Big River (Appendix B and Fig. 17, location Y-136); (2) a 7-m-thick section SE of the caldera rim in the saddle between the Eastern Edifice and Dome 2315, where the ignimbrite overlies intact fallout (3–13 cm thick) and where ferrocreted slabs of ignimbrite 10–40 cm thick scattered on the surface suggest that the top of the primary surface is locally preserved (location Y-131); and (3) a 12-m-thick section of mostly massive ignimbrite exposed in a gully along the north toe of the Northern Edifice, on the right bank rim of the narrow gorge of Big River, 2.75 km NW of the center of the caldera (Y-126). There, the ignimbrite rests on 3 cm of fallout, which in turn rests on 1–6 cm of organic-rich soil developed atop the irregular blocky surface of the Big Breccia deposit. As discussed above (Section 6), this soil is well dated at 6010 ± 100 ^{14}C yrs B.P. (Fierstein, 2007) and constrains the elapsed time between the preceding dome disruption (Big Breccia deposit) and the ~5800 ^{14}C yrs B.P. caldera-forming event to ~200 years.

Pumice clasts in the ignimbrite are typically white, buff or grey, a small fraction are nearly black, and sparse black/white banded pumices are found in many locations (Appendix B). Pumice clasts range from 61 to 66% SiO_2 (Fig. 5) and most, but not all, are distinctively coarsely vesicular and full of dark elongate crystal clots (blebs) like those in the fallout pumice. The more finely vesicular, clot-poor subordinate pumice is also present. Lithic clasts are mostly glassy, grey, crystal-rich dacite lava, although orange-altered clasts are a minor component at all locations sampled, and sparse Jurassic basement clasts are also present. The ignimbrite matrix, typically dark grey-brown to light lavender-grey, is sandy or gritty to touch and coarser than many pumiceous ignimbrites, which commonly have a high fraction of very fine ash (Walker, 1971; Fierstein and Hildreth,

1992). This may in part be due to significant contributions by comminution of glassy, friable dome rocks as main lithics.

Lithic and pumice concentration zones, most common in the upper half of thick ignimbrite exposures, are typically no more than two meters thick. Large pumice clasts in these horizons range from 10–50 cm, with some as large as 85 cm. In the LCZs, lava clasts are 10–60 cm, with some to ~100 cm. However, one location 2 km NW of the rim exposes a 20-m-thick lithic lag breccia intercalated near the top of the ignimbrite (where the entire section is >45 m thick) in which lithic clasts are as large as 2 m. The location is where Big River now makes a nearly 45-degree bend from ~NNE to ~ENE and is channeled into a narrow gorge (Fig. 1; location Y-100). Just downstream along the northeastward stretch of the river are several exposures of a similar, but thinner (2 m), LCZ. During emplacement at least some of the ignimbrite must have taken a similar flow path, directed first west to northwestward out of the vent, then following the drainage NNE to where it was turned northeastward by pre-existing topography. Such accumulations of thick lithic breccias on the inner bends of curving valleys are seen in pyroclastic flow deposits from Laacher See volcano. There, they have been interpreted by Freundt and Schmincke (1985) as due to a flow vortex which remained stationary near the inner bend of the valley, or diminishing velocities outward toward ignimbrite margins as the moving flow navigated a curving path, with successive pulses of flow contributing large lithics as each passed by that spot. This implies that a large volume of 'normal' ignimbrite flowed past this point, losing lithics but continuing downstream. Alternatively, if the ignimbrite came straight down the north slope of the North Edifice, the break in slope would likely precipitate dumping of large lithics there, as well, although this is not found (or exposed) at the base of steep slopes elsewhere.

In contrast to the lithics elsewhere in the ignimbrite, the lowest 3 m of this 20-m-thick lithic lag has a significantly larger fraction (~30%) of yellow-orange crystal-poor altered lava clasts (with pyrite). The only exposure of such rocks in the caldera wall is in the oldest component of the Eastern Edifice. This suggests a large failure or mining out of the Eastern Edifice late in the eruptive sequence.

8.3. Eruption volumes

Eruption volumes are poorly constrained for this caldera-forming event due to patchy preservation and/or exposure. Thickness measurements, maximum pumice (MP) sizes, and median grain size (Md) are shown in Fig. 17 for all sites where intact fallout was found. Deposits within 10 km of vent are all pumice falls, shed from (what was likely) a (sub)plinian column. Beyond 25 km from vent, the fallout is a fine-grained bright orange layer that is largely coignimbrite ash. Thickness data used in volume calculations (after Fierstein and Nathenson, 1992) yield an estimate of ~0.3 km^3 within the moderately constrained 9-cm isopach and another 0.4 km^3 within the less well-constrained 3-cm isopach. Although distal ash distribution is poorly constrained, we draw tentative isopachs to 1.5 cm that include the well-correlated tephra on the Kenai Peninsula and the less well-correlated tephra on Afognak Island and Kukak Bay (Fig. 1; see Section 8.1.3). This could add as much as 2.8 km^3 to the fall volume, for a total tephra fallout volume of as much as ~3.5 km^3 (~1.5 km^3 DRE).

Exposures in the Big River and South Kaguyak Creek drainages suggest that at least 115 km^2 around Kaguyak caldera were covered by pyroclastic flows to some depth, and the flows probably thinned toward the coast. Because the ignimbrite base is rarely exposed, this volume, too, is poorly constrained. Crude volume calculations of on-land ignimbrite can be made by assuming average outflow thicknesses of 10 m, 15 m, and 20 m, which yield between 1.1 and 2.3 km^3 , respectively. This latter is a maximum volume, since preserved (and exposed) ignimbrite thicknesses vary greatly, being thin atop the caldera rim and thick in the river gorges. In addition, the ignimbrite likely flowed some distance offshore, but we have no constraints on

that volume and it is not included. Thus estimated, total eruptive volume, including fallout and ignimbrite, is at least 1.8 km^3 and no more than 6 km^3 (as tephra) or 0.8 to 2.5 km^3 DRE.

Subsidence volume of the caldera can also be calculated using an average rim elevation of 500 ft (150 m) above lake level, an average lake depth of 150 m (based on measured depths, see Section 11), and a measured 4.1 km^2 for the area of the lake. This yields a volume for the caldera of $\sim 1.2 \text{ km}^3$ (DRE), which is a minimum subsidence volume because it excludes any intracaldera ignimbrite beneath the lake.

8.4. Postignimbrite sedimentation

Many exposures of the ignimbrite in the Big River drainage area are directly overlain by stratified sediments ubiquitously yellow-orange in color due to fumarolic alteration and locally ferrocreted, suggesting in-situ alteration due to ignimbrite degassing. An especially thick sequence (near Y-3; 6 to 10 m) exposed in a large gulch NW of the caldera is made up of cross-bedded, crystal-rich sediments with few clasts $> 1 \text{ cm}$. Nearby (Y-135), the sediment sequence begins with a 4–6-m-thick, blue-grey mud directly on top of the ignimbrite, in turn overlain by orange sediments fine-grained enough that compacted layers break apart and form small chips on the sloughed slopes. Exposures just beyond the preserved or exposed ignimbrite margins include thick blue-grey pumice-bearing mud intercalated with pumiceous debris flows. Such deposits are seen in the flat terraces near the headwaters of Big River (NW of the caldera) and near the junction of the north and main forks of Big River (NNE of the caldera). In the lowlands near the Kaguyak coastline (Y-106, 107), hyperconcentrated sand flows (hcs) make up a significant portion of the exposures. At least several meters of hcs—some massive and some slightly stratified, and all with plenty of small rounded pumice lapilli—are overlain by cobble alluvium and fine blue-grey mud with intercalated layers and lenses of pumiceous debris flows. The base of these deposits is not exposed here, and neither is any primary ignimbrite.

Lack of soil or other deposits between the primary Kaguyak ignimbrite and its derivative secondary sedimentary deposits show clearly that ponding of the surrounding drainages and reworking of

the primary ignimbrite deposit ensued immediately post-emplacment. Moreover, widespread alteration of the overlying secondary deposits are good evidence that the ignimbrite remained hot and degassing for months or years after it came to rest, with some of the alteration also due to precipitation of iron and silica from warm groundwater.

9. Postcaldera eruptions

Two postcaldera domes are exposed above today's lake level within the caldera (Figs. 2, 3). The larger one, 1000 m across at lake level and rising 240 m above the water surface, impinges on the SW corner of the caldera (butting up against the thick coulees of the Southern Edifice in the caldera wall) and is made up of four lobes that range from 63–64% SiO_2 (Fig. 5). The other dome is slightly less silicic ($\sim 62\% \text{SiO}_2$) and rises only 30 m above the water surface, forming a 200-m (in diameter)-island near the middle of the lake. The two domes likely overlap underwater, since measured water depth between the two is only 24 m (see Section 11). The lavas are all crystal-rich (~ 20 – 40%) and plagioclase-dominant with $\text{opx} + \text{cpx} + \text{oxides}$ making up the mafic suite (Appendix A). In contrast to the nearby precaldern thick coulees of the Southern Edifice, almost no large mafic phenocrysts and no hornblende are present in these postcaldera edifices. Although the fraction of mafic phenocrysts is variable ($\ll 1\%$ to $\sim 4\%$), they all tend to occur as clusters of small (1-mm) crystals, the clusters common in the post-caldera dome lavas as big as 5 mm. These crystal clusters are similar to (though not as large as) those common in the pumice of the caldera-forming eruption.

Also post-caldera is an orange fragmental (probably phreatic) deposit with patchy distribution around the rim. It overlies the ignimbrite as exposed in gulches on the NW flank of the caldera and mantles the Big Breccia deposit and swales cut into that deposit along the NE, NW, W, and SW caldera rim. The unit is as thick as 5–8 m in the low NW saddle where typical large clasts are decimeters in scale to as much as $\sim 2 \text{ m}$, but in the NE notch, the deposit is thinner (2–3 m) and not so coarse (clasts to only 20 cm). Poorly sorted, the deposit has a sandy matrix that includes enough clay to cause clumping, and it is orange owing to comminuted hydrothermally altered and ferrocreted material. Although the deposit includes a small fraction of fresh grey lava clasts, most are thoroughly hydrothermally altered dacite and Fe-

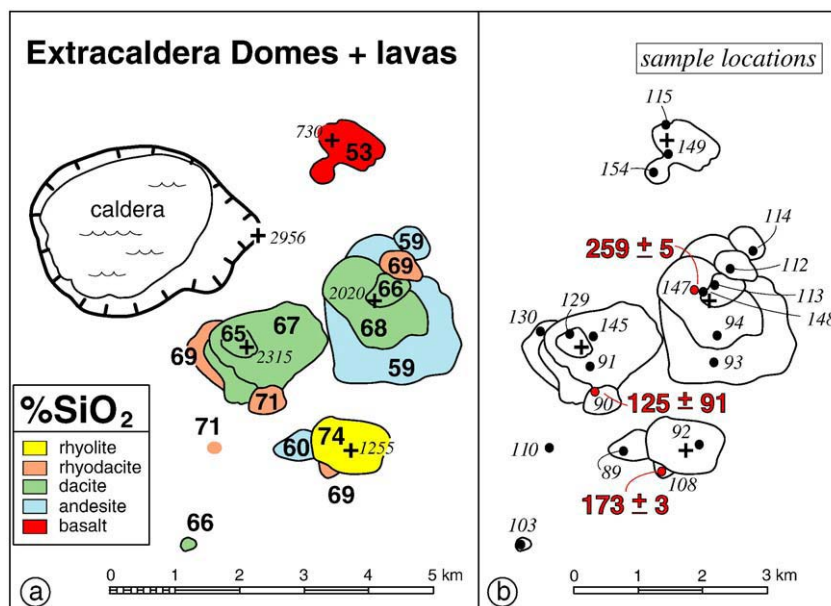


Fig. 19. (a) Extracaldera dome clusters and lavas colored according to composition. Bold numbers are SiO_2 -contents: Rhyolite ($\geq 73\% \text{SiO}_2$); rhyodacite (69–72% SiO_2); dacite (> 63 – $68\% \text{SiO}_2$); andesite (54–63% SiO_2); basalt ($\leq 53\% \text{SiO}_2$). The unnamed clusters are referred to by their summit elevations in feet (summits marked by a “+” and elevations in italics). (b) Sample locations marked by filled black circles and labeled in italics (“130” is Y-130). Red filled circles mark dated samples, with $^{40}\text{Ar}/^{39}\text{Ar}$ date in red. Samples Y-103 and Y-110 are isolated outcrops of eroded lava flows largely buried by the Kaguyak ignimbrite.

encrusted sand, granules and lava clasts; little or no pumice is included. Very common are ferrocreted stratified sediment and agglutinate (lava) clasts. The former are typically preserved as hard plates of graded lake bed sediments that presumably accumulated on the caldera floor, then were disrupted by explosions that accompanied emplacement of the post-caldera domes. A lag deposit is preserved only locally along the SW rim, where scattered plates of ferrocreted lake sediments are up to 50 cm across and 5 cm thick. Some of this orange deposit is also preserved at the top of large postcaldera Dome 2015, but not atop the island dome, which suggests that at least part of the phreatic deposit was related to explosions associated with emplacement of the latter.

How soon after caldera collapse the postcaldera domes were emplaced is uncertain, but a few observations provide some constraints, including:

- 1) the orange clay-bearing deposit found mantling the caldera rim also coats the top of larger Dome 2015, implying that the island dome is the younger of the two;
- 2) plate-like clasts of hydrothermally altered lake sediments included in the orange phreatic deposit suggest enough time elapsed after caldera collapse that a shallow lake formed, sediment accumulated and was hydrothermally altered.

10. Extracaldera domes and lava remnants

Four extracaldera dome clusters that erupted within the quadrant northeast to southeast of the present caldera span the entire compositional range (53% to 74% SiO₂) of the Kaguyak dome field (Fig. 19). None of these clusters is named, so we refer to them by their summit elevations in feet as marked on the USGS topographic maps (for example, *Knob 730*). Three of them—all within 1.5 to 3.5 km southeast of the Eastern Edifice (Fig. 3)—span wide compositional ranges (Fig. 19). Only Knob 730, 2 km northeast of the Eastern Edifice summit, is fairly homogeneous (53–54% SiO₂). All of the domes share the low-TiO₂ compositional signature common to Eastern Edifice lavas (Fig. 5c), all have been glaciated, all are older than the rest of the dome field except for older parts of the Eastern Edifice, and all are part of the early phases of Kaguyak dome-field building. Present-day volumes of these domes have been estimated, recognizing that unknown fractions have been eroded away. Easterly Dome 2020 (~770 million m³) and southerly Dome 2315 (~490 million m³), both about the Eastern Edifice, and they are an order of magnitude bigger than outlying Dome 1255 (70 million m³) and mafic Knob 730 (40 million m³). These estimates provide a minimum total volume of 1.4 km³ for the extracaldera domes, all of which have been glacially scoured.

10.1. Knob 730

Most mafic of all Kaguyak eruptive products (53–54% SiO₂), Knob 730 is a small flat hill of dense, black lava 2 km NE of the caldera rim (Figs. 3, 19). One hundred twenty meters of relief on the steep NE face exposes steeply inclined slender columns, suggesting emplacement against ice. Another small ridge just uphill is similarly mafic and, although erosionally separated from the main knob, is part of the same magma batch and is clearly overlain by Eastern Edifice lavas. The knob itself may have been a small dome with the uphill ridge a remnant fissure vent. Though exposure is poor, it seems more likely that the two are remnants of an glacial lava flow from a vent now concealed by the pile of

younger Eastern Edifice lavas. The original configuration of this unit is poorly constrained, but we assume that most of it is buried beneath younger flows or eroded by ice. Another mafic lava remnant 2.5 km north, on the opposite side of the Big River valley, might be a remnant of this flow (see Section 10.5).

Distinctly fine-grained, Knob 730 is characterized by phenocrysts typically no more than ~1 mm (pl>opx>cpx; Appendix A). There is no hornblende, but there are many sub-mm olivine microphenocrysts in various states of resorption, thus joining the youngest sequence of the Eastern Edifice and some of the youngest lavas of the Southern Edifice as the only eruptive units here to include olivine. Efforts to date this lava have been unsatisfactory largely owing to its very low K₂O (0.2–0.3%) content. Mapping suggests this unit was emplaced between Eastern Edifice eruptive packages 1 and 3 (300 and 60 ka).

10.2. Dome 2020

Five overlapping or contiguous eruptive units that range from 59% to 69% SiO₂ built Dome cluster 2020, the high point of which lies only 2 km SE of the summit of the Eastern Edifice (Fig. 19). Two of these units are large (~300 to 400 million m³) and three small (~15 to 40 million m³). The two oldest, both 59% SiO₂, include a small dome at the NE edge of the complex (Y-114) and a large coulee (Y-93), atop which the other three eruptive units were piled. Exposed in the steep wall beneath the small dome is an isolated remnant of a thick buff-colored ignimbrite, assumed to be of pre-Kaguyak age (Fig. 20a).

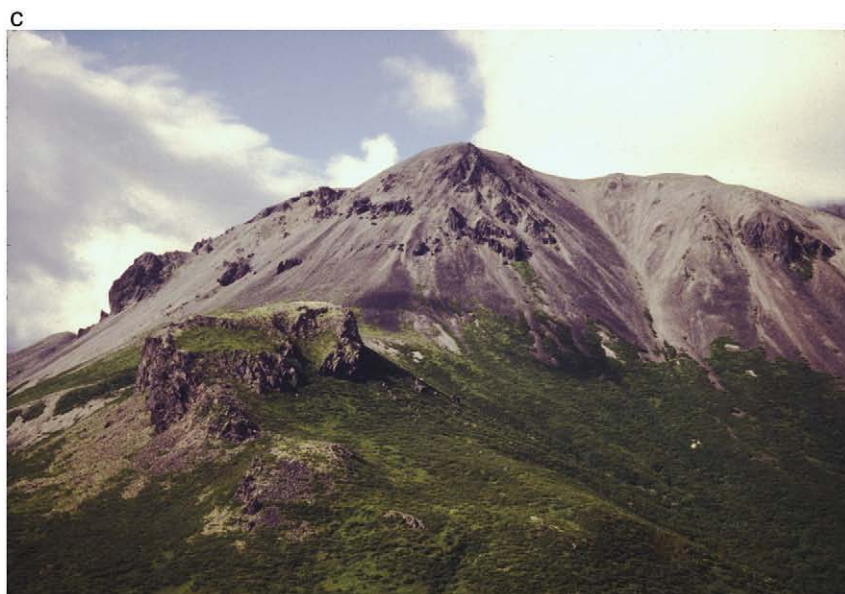
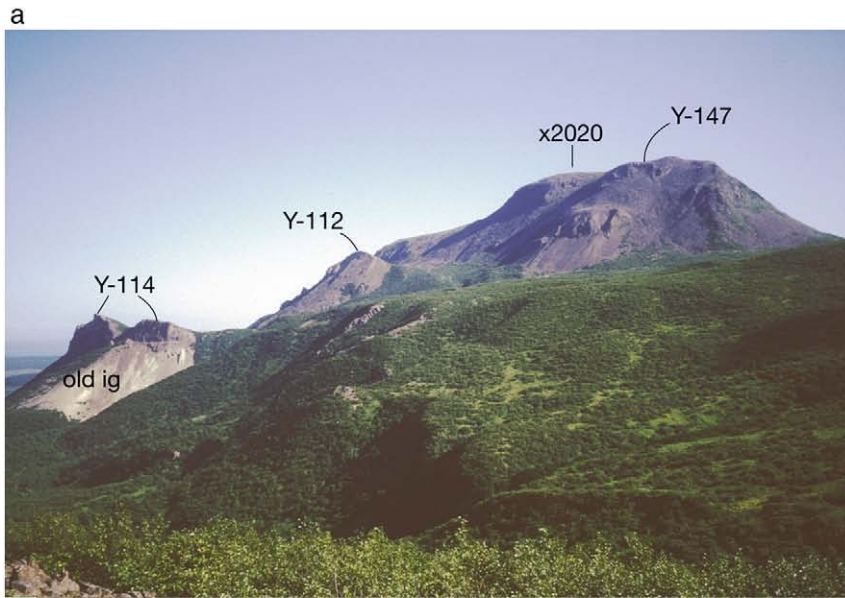
Another small dome adjacent to the first small one, but with 69% SiO₂ (Y-112), is the only eruptive unit of this dome complex to contain hornblende, with conspicuously lower TiO₂ and higher MgO than the other dacitic units in this complex (Fig. 5). Another large effusion built the main elongate dome (68% SiO₂; Y-94 and 147), which is flow-banded and rises above the flat shelf of the initial dome. The capping flow, 66% SiO₂, (Y-113, 148), extruded from the center of the previous one and forms the high point of the composite dome complex. All components have as much as ~15% plagioclase which tends to be small (1–3 mm) and few mafics (opx+cpx±FeTi oxides), which also tend to be small (≤1 mm). Only the NE-most dome is crystal-richer (~35% phenocrysts), but its mineralogy is similar to the others, except that the most silicic of the domes also includes minor hornblende and a rare resorbed biotite.

There is no systematic progression of composition or volume in emplacement of the five dome components, and no evidence for much erosion between them. An ⁴⁰Ar/³⁹Ar date on one dome (Y-147), essentially representing the middle of the pile, yields 259±5 ka (Table 1).

10.3. Dome 1255

Together, the three components of Dome cluster 1255 (Fig. 20b) total only ~70 million m³—much less than either of its neighbors—but they span much of the compositional range of the entire Kaguyak dome field. The central main dome is an elongate ridge of crystal-rich rhyolite lava (74% SiO₂; Fig. 19) that retains at least some of its micropumiceous carapace on top but has a glaciated, sheer 240-m north face (Fig. 20b). A subdued smaller shoulder to the west is a greenish, weathered, crystal-poor andesite (60% SiO₂) with only 300 feet of relief and is clearly beneath the larger, younger dome.

Fig. 20. Extracaldera dome clusters that predate caldera collapse. (a) View SSE of Dome cluster 2020. Small dome (Y-114) overlies a 90-m bluff of pale pre-Kaguyak ignimbrite (old ig.) ~1 km east (left) of summit of main cluster. Small dome (Y-112) is at the east foot of the main cluster and summit (×2020) is the youngest component erupted atop the slightly older Y-147 dome. (b) View south of Dome cluster 1255, toward 240-m glaciated scarp of main rhyolitic dome and subdued older andesitic shoulder (far right). Lowland beyond the dome cluster is ignimbrite-filled South Kaguyak Creek. Foreground is platform of oldest lavas of Dome 2020 cluster and skyline ridge is Mesozoic sedimentary basement. Helicopter for scale (far left, center). (c) View N toward Dome cluster 2315. Flat-topped rhyodacite knob Y-90 is in front of the main pile of four units that largely overlap.



Glaciers have eroded this shoulder strongly enough to expose a platy interior. Smallest of all is a crystal-rich rhyodacite nubbin (69% SiO₂) that peeks out from under the southern foot of the main central dome. Distinctively white with large altered opx to 5 mm, this is the only extracaldera dome rock in which we have noticed coherent more mafic blobs. Both silicic units contain quartz, more orthopyroxene than clinopyroxene, and a little hornblende (Appendix A). The andesite includes plagioclase and both pyroxenes (no hb), but all the mafics are strongly resorbed. The vesicular surface of the main dome contrasts with the exposed platy interior of the western shoulder, raising the possibility that the latter is very much older. The rhyodacite nubbin, however, yields an ⁴⁰Ar/³⁹Ar age of 173 ± 3 ka (Y-108; Table 1), showing that the two younger units of this cluster are considerably younger than its northern neighbor, Dome 2020.

10.4. Dome 2315

Dome cluster 2315 is a 0.5-km³ pile of five silicic eruptive units, 65 to 71% SiO₂ (Fig. 19). Four of these largely overlap in a stack centered near the present high point ×2315, the vent for the youngest of them. Rising steeply 1600 feet on the SE flank to a triple-humped summit area, the lava pile borders a shallow valley on its opposite flank where it abuts the Eastern Edifice. In this trough is one of the few places the base of the caldera-forming ignimbrite is exposed (see Section 8). Only the most silicic eruptive unit (71% SiO₂; Y-90) vented separately from the rest; it forms a flat-topped knob rising steeply ~150 m to a low saddle on the south side of the main dome (Fig. 20c). The lava dips 25° away from the saddle and appears to have been extruded in place as the youngest component of this dome complex.

Compositions of Dome 2315 lavas are similar to those that erupted over a wide age range (from ~300 to 60 ka) at the adjacent Eastern Edifice. Only the youngest Eastern Edifice lavas (package 4), all <65% SiO₂, have no compositional equivalent in the Dome 2315 pile (Fig. 5). There is no simple compositional evolution with time, however, with either the Dome 2315 or the Eastern Edifice lavas.

Phenocrysts in Dome 2315 lavas indicate a mixed magma history. Most units have plenty of phenocrysts, the oldest has fewer, but in all plagioclase dominates and mafics (opx, cpx, and mt) are few (Appendix A). Hornblende is present only in the most silicic dome (Y-90), in which it is the dominant mafic phase, olivine in various stages of degradation is present in the main dome unit (Y-91), and at least a trace of quartz is present in all the lavas. Though quartz phenocrysts are subhedral in the youngest rhyodacite (Y-90), quartz in all the other units is rounded, embayed, or corroded. Corroded remains include vesicles lined with clusters of tiny pyroxene crystals (mostly opx, some cpx) and pockets of light brown glass, to rings of cluster pyroxenes enclosing vesicles with partly preserved quartz phenocrysts. These are similar to jacketed quartz phenocrysts described in contaminated basalts (Webb 1941; Doe et al., 1969; Bacon and Metz 1984). In contrast to the subhedral and fairly clean phenocrysts of the rhyodacite dome, phenocrysts in the rest of the lavas of this dome complex vary in preservation state (resorbed, clean, zoned), include non-equilibrium assemblages, crystal fragments, and crystal clots with phenocrysts different from the cognate magma (in size or type). Such textures, in particular the jacketed quartz phenocrysts, reflect a complex mixing history.

Dating these lavas directly has been unsuccessful. Glassy groundmass and very low-K plagioclase has precluded reliable results, even from the rhyodacite lava, Y-90, which yielded a ⁴⁰Ar/³⁹Ar age with a large error (125 ± 91 ka). Relative ages with neighboring Dome 2020 are also uncertain due to poor exposure. Only the glaciated scarp at the east end of the valley between the Eastern Edifice and Dome 2315 shows a juxtaposition of lavas from those two centers. This exposure suggests the latter is banked against the older part of the former, thus that Dome 2315 is younger than Eastern Edifice package

2, which in turn suggests an age younger than ~200–150 ka for Dome 2315. Little evidence for long erosional breaks between emplacement of any of the components of this dome (except between the small rhyodacite dome and the rest), implies that most of this dome complex was emplaced within a confined eruptive period which we infer postdated emplacement of Dome 2020 (~260 kyr) and the early phases of the Eastern Edifice (~200–150 kyr), and predated the active dome-building period at the Southern and Northern Edifices 30 kyr ago.

10.5. Lava outliers

Remnants of three different lavas are preserved atop a wide, glacially-carved bench that rises as much as 240 m above the north wall of Big River, 5 km NE of the caldera, and two additional (and different) remnants are exposed through the ignimbrite and vegetation cover in the low area south of the caldera in South Kaguyak Creek (Fig. 3). All are glaciated and have the low-K characteristic of the Kaguyak suite (Fig. 5), but they range from 54 to 71% SiO₂. We considered the possibility that the remnants along Big River came from nearby Fourpeaked Volcano (Fig. 1), but these remnants have much lower K₂O than Fourpeaked lavas at a given SiO₂ content, and the drainage pattern does not provide an obvious route for such a source. We conclude that each of these remnants originated from the Kaguyak field itself. Because each remnant is different mineralogically and chemically, we discuss them separately.

10.5.1. Big River basalt bench

A mafic lava remnant (Y-116; 54% SiO₂) on the left bank of Big River is perched atop the SE end of a 6.5-km-long ice-scoured bench carved out of the sedimentary Jurassic basement rocks exposed widely in the area (Fig. 3). The lava is 120 m thick and columnar throughout, has a smooth glacially scoured surface and is massive to the top, with no upper flow breccia preserved. The only other Kaguyak lava as mafic as this one is situated nearly due south across the 2.75-km-wide glacial valley where basaltic Knob 730 (53–54% SiO₂) and adjacent related ridge (at 240 m elevation) protrude from beneath the apron of Eastern Edifice lavas. The Knob itself is a flat-topped smaller version of the plateau on the other side of the river, as high as 300 m elevation, and is of similar thickness to the lava remnant across the valley. Mineralogically similar (though not identical), both lavas have a microlitic groundmass with many sub-mm olivine phenocrysts sprinkled throughout, some larger olivine and plenty of clinopyroxene and orthopyroxene phenocrysts. Although the Big River lava remnant is slightly finer-grained with fewer phenocrysts and crystal clots than the Knob samples, these lavas are compositionally so similar to one another and different from all other lavas in the area (Fig. 5) that the two are likely to represent the same eruptive episode.

Although dating experiments on Knob 730 were unsuccessful, the Big River remnant (K₂O=0.2–0.3%) yields a precise ⁴⁰Ar/³⁹Ar age of 121 ± 12 ka. Knob 730 and the mafic bench are probably remnants of a larger lava flow stripped from the Big River valley during the last major glacial episode.

10.5.2. Big River andesite bench

One kilometer west of the mafic lava just described is a 1500-m-long remnant of another lava flow (Y-118), ~60 m thick with its base ~180 m above the present valley floor (Fig. 3). This unit is silicic andesite (62% SiO₂) with at least 50% phenocrysts (pl+hb—a few as large as 7 mm, plus minor cpx+opx+mt). Though the lava is rusty stained and altered, the hornblende crystals are not thoroughly black, suggesting that much of the degradation is post-emplacement and not syneruptive.

Mineralogically dissimilar to products of the Eastern Edifice, which all lack hornblende, this lava is similar to several from the Northern, Southern, and Central Edifices, all of which include crystal-rich flows

with a mafic phenocryst assemblage dominated by hornblende and orthopyroxene. The nearby Northern Edifice is the most likely source. Compositionally, however, the Big River andesite remnant is more silicic than any Northern Edifice lavas exposed in the caldera walls and has lower TiO₂ and higher MgO higher contents than the trend for the Northern Edifice suite (Fig. 5). Compositional similarities are greater with some of the Southern Edifice flows, except for TiO₂, which is as low as that in the Eastern Edifice suite. Moreover, access of Southern Edifice flows to the Big River drainage is conceptually difficult, especially because the Central Edifice (which predated the Southern one) would have blocked the most direct flow route (north to north-eastward). The Central Edifice, then, would seem a more likely source for this lava remnant. In contrast to the phenocryst assemblage, however, low-TiO₂, low Zr and high La/Ce suggests the magmatic source for this lava remnant has more affinity with the Eastern rather than the Central Edifice (Figs. 5, 14, Appendix C). This outlier lava has characteristics that suggest affinity to both the Central and Eastern Edifices, but are not exactly like either. The lava could be a remnant of an older eruptive phase not represented in the present caldera wall.

10.5.3. Big River Knob 1015

An oblong-shaped andesitic knob (Y-117; 56% SiO₂) with a small pond on top and spectacular sets of long vertical to inclined slender columns throughout, sits on the glaciated plateau bench behind the Big River andesite remnant described above (Figs. 21, 3). Partly glassy, with 10–15% plagioclase phenocrysts (1–2-mm) and minor olivine (mostly sub-mm) in a microlitic groundmass, with irregular vesicles and no alteration, this is decidedly unlike the altered hornblende-bearing lava remnant just 100 m away, and also unlike the basaltic remnant at the SE end of the plateau. Moreover, this lava is compositionally different from all other flows preserved at Kaguyak in that it is chemically intermediate between the mafic lavas of Knob 730 (53–54% SiO₂) and the least silicic of the Northern Edifice lavas (58% SiO₂; Fig. 5). Only the five analyzed enclaves (3 from Southern Edifice flows, 1 from a Central Dome flow, and 1 from a clast in the Big Breccia) are mafic andesites (56–58% SiO₂) comparable to Knob 1015. Compositional affinity seems greatest with mafic lavas of the Eastern Edifice, including low TiO₂, high MgO and La/Ce (Fig. 5, Appendix C) and olivine as a common mafic phenocryst.

Age and source of this lava remnant are unknown. A regional map by Riehle et al. (1994) marks this as a vent, but—although the pond at the top suggests a crater morphology—there are no ejecta, fragmental deposits, or alteration. The oblong shape and steep walls suggest tuya morphology—but we did not see hyaloclastites, tuffs, or pillow lavas that are common features at tuyas elsewhere (Mathews, 1947; Allen et al., 1982). The ubiquitous slender columns do suggest extrusion as a subglacial dome. If this is a vent, the fresh lava suggests it is younger than the adjacent altered hornblende-lava remnant. Alternatively, this could be a slightly more evolved flow related to the eruptive episode of Knob 730, with affinity to nearby basaltic remnant Y-116. The nearly circular morphology and summit depression must then be attributed to glacial erosion and, because the mafic andesite is at a higher elevation than the hornblende-lava remnant, the former is likely to be older. We have no dates that could help resolve this uncertainty.

10.5.4. South Kaguyak Creek rhyodacite

An isolated lava knob 25 m high makes a prominent nose along the middle fork of South Kaguyak Creek ~1.5 km SSW of Dome 2315 (Fig. 3; Y-110). Pale grey, with ~10% plagioclase phenocrysts plus small mafics (opx>cpx>mt), this rhyodacitic lava (71% SiO₂) does *not* have the low-TiO₂-signature of the nearby Eastern Edifice or extracaldera Domes 2315 and 1225 (Fig. 14). Instead, the rhyodacite remnant is more on-trend with lavas of Dome 2020, and has higher values of TiO₂, Zr, Ba, and Nb, even compared to the most silicic lavas of the Eastern Edifice and the other extracaldera domes (Fig. 14, Appendix C). Clearly not affiliated with the low-TiO₂-clusters, and so isolated from Dome 2020 that it seems implausible to have vented there, the South Kaguyak Creek rhyodacite is likely to be a remnant of an older lava flow from a now-buried or eroded source that predates at least part of Dome 2315.

10.5.5. South Kaguyak Creek dacite

Another knob, 50 m high along the southernmost fork of South Kaguyak Creek (Fig. 3; Y-103), is a remnant of a thick, glaciated, glassy intracanyon dacite lava (66% SiO₂) with several tiers of subhorizontal to inclined columnar joints that suggest multiple flow pulses. Weathered dark grey-brown surficially and fairly brown internally, the outcrop looks quite old. The phenocrysts, however, (pl>hb>relict opx>cpx+trace quartz) tend to be fairly clean; only the orthopyroxene is strongly

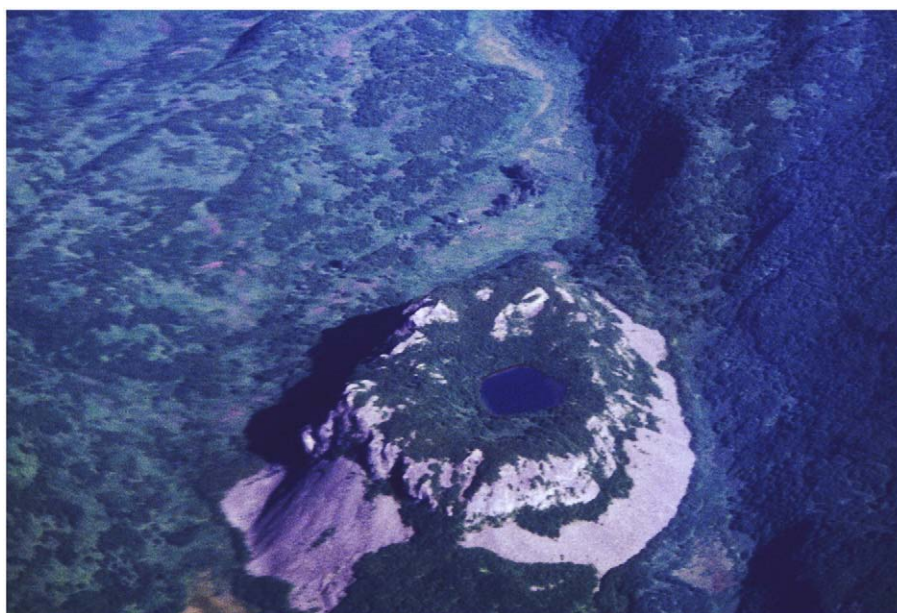


Fig. 21. Aerial view of Big River Knob 1015, which is ~35 m high, 300 m across and 600 m long. Pond on top suggests a crater morphology, but the Knob is columnar-jointed throughout with no fragmental deposits. Here shown nestled next to vegetation-covered steep margin of elongate andesite lava outlier (Y-118, Fig. 3) to the SW (right of Knob).

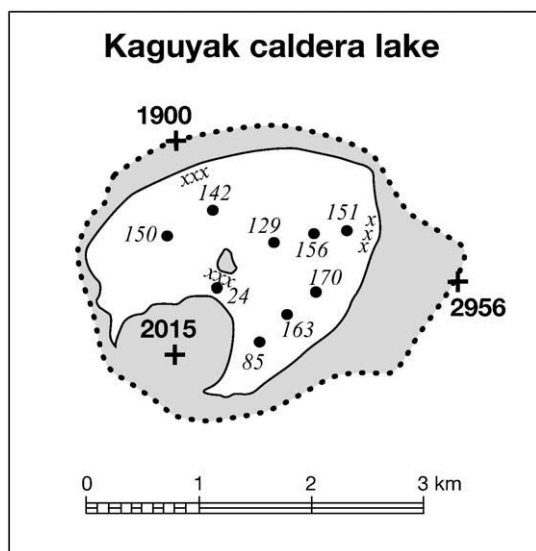


Fig. 22. Kaguyak caldera lake (white) with water-depth measurements in meters (locations marked by filled circle, depths are italicized; e.g., “150”); lake elevation above sea level is 1200 ft. Caldera rim is dotted with high points (in feet) marked by “+”; Northern Edifice summit (1900 ft); Eastern Edifice summit (2956 ft); top of intracaldera dome cluster (2015 ft). Locations of gas bubbling marked by “xxx”.

resorbed. Similar to the rhyodacite remnant described above, this dacite lava remnant has clearly higher values of TiO_2 , Zr, Ba, and Nb than any of the lavas from the Eastern Edifice and from Domes 2315 and 1255, and must have originated from a source now buried or eroded.

11. Caldera lake, gas seeps and shoreline precipitates, lakewater chemistry

Kaguyak caldera lake is 2×2.5 km across (Figs. 2, 3). Lake depth was measured on calm days in July, 1999 from an inflatable boat at nine locations by reeling overboard a long spool of nylon cord attached to a bag of rocks. Attention was given to keeping the cord vertical to avoid overestimating water depth. Most measurements were between 130 and 170 m (Fig. 22), with shallower spots near the intracaldera domes. Surface water temperatures, measured at each of these locations, were consistently between 4° and 5°C . An approximate lake volume of 0.5 km^3 is calculated assuming 150-m average lake depth.

11.1. Gas seeps and shoreline precipitates

Gas seeps bubbling up to the caldera lake surface were seen in three locations in July of 1999—along the north lakeshore, east lakeshore, and on the SW shore of the small island in the middle of the lake (Fig. 22). Those to the north cover a roughly linear area from the shoreline to ~ 75 m offshore with isolated sporadic bursts of clustered bubbles. Typically ~ 40 – 50 such clusters were visible at a given moment, although as many as a few hundred sites in all were active over this limited zone. A stretch of ~ 75 m of the adjacent shoreline talus is stained with white, yellow, pale orange, and black precipitates, and white precipitates can be seen on rocks deep down in the clear water. X-ray diffraction (XRD) shows the dominant precipitates and alteration products to be silica, clays (mostly montmorillonite), alunite, goethite, hematite, and a little celadonite. An H_2S odor is conspicuous near the shore where the water is 1–2 m deep, but the bubbles seem odorless out in deeper water (presumably scrubbed of S, leaving only CO_2 ; Symonds et al., 2003).

Bubbles were similarly vigorous with an H_2S odor along a short stretch of the east shoreline (Fig. 22) and not quite as vigorous but with a strong H_2S smell at the SW foot of the island dome. Both locations are marked by white precipitates on the shoreline talus.

11.2. Lakewater chemistry

A surface water sample collected in the middle of the lake (Table 2) is chemically similar to one collected ten years earlier by Cameron and Larson (1992). Although our sample was collected ~ 300 m due east of the island dome, away from shorelines and gas seeps, elevated Cl, SO_4 , SiO_2 and B values are similar to those measured in lake water with bubbling gas near The Gas Rocks and in seeps near Ukinrek Maars south of Becharof Lake (~ 165 km to the SW of Kaguyak; Evans et al., 2007). In comparison, the lake filling Katmai caldera—magma storage site for the 1912 plinian eruption—had much higher SO_4 , SiO_2 and B values as measured by Motyka (1977). Comparison of chloride and sulfate values in Kaguyak caldera lake with surface water samples from a large area of southeastern Alaska, as reported in the USGS National Water Information System (NWIS), virtually require hydrothermal input since evaporative concentration of solutes in the lake is ruled out by δD and $\delta^{18}\text{O}$ data (Table 2). High Cl/Br (~ 515) is also typical of volcanic or hydrothermal contributions, as is the measured pH of 5.5 (reported values for surface waters range from 6.2 to 7.7 in the NWIS). Kaguyak Cl and SO_4 values are intermediate between typical surface waters and hot springs, probably reflecting the balance between precipitation and the hydrothermal input to the lake. Although additional measurements are needed to refine flux estimates, preliminary calculations suggest that input of hydrothermal Cl at ~ 200 tonnes per year would maintain a steady-state Cl concentration of 40 mg/L (Table 2) indicating continued hydrothermal input to the caldera lake (W. C. Evans, USGS, personal communication).

12. Discussion of eruptive history

Volumes of the Kaguyak dome clusters have been calculated as (a) those preserved and as (b) conservative reconstructions of original (pre-erosional) extents of each. Although erosion and caldera collapse make many estimates rather uncertain, the resulting “minimum” and “maximum” cumulative-volume curves are similar in shape (Fig. 23). Most of the 15 increments represent composite extrusions that built

Table 2

Chemistry of Kaguyak lake and other volcanic lakes and seeps and surface waters in Alaska (in ppm)

Location	Kaguyak Lake	Kaguyak Lake	Becharof Lake	Ukinrek Maars	Katmai Lake	Katmai Lake	Surface waters*
Collector	(F+H)	(C+L)	(Evans+)	(Evans+)	(Motyka)	(Motyka)	(NWIS)
Li	0.16		0.048	0.010	0.92	1.2	
Na	39	40.99	23	37	760	590	
K	5.21	5.27	1.1	3.8	90	110	
Mg	5.96	6.45	3.0	13	51	62	
Ca	9.56	11.16	10	60	300	300	
F	0.09		0.04	0.22	0.9	1.1	
Cl	41.2		42	47	1350	1750	6.0
Br	0.08		0.11	0.16			
SO_4	54.2	54.53	6.8	73	1250	1200	8.9
HCO_3	35.1		27	179			
SiO_2	44.1	42.8	1.1	24	120	140	6.8
B	0.87		0.39	<0.2	12	14	
δD	-89.2		-77	-84			
$\delta^{18}\text{O}$	-11.71		-10.2	-10.9			
pH	5.5				2.5 to 3.0	2.5 to 3.0	6.2 to 7.7
Surface T° ; C	5		8.6	7.8	5.8	5.8	

Notes: Kaguyak caldera lake water collected by Fierstein and Hildreth (F+H) in July, 1999; analyzed by C. Janik, U.S. Geological Survey, Menlo Park, CA. Cameron and Larsen (C+L; 1992) collected Kaguyak Lake in 1988; Evans et al. (Evans+; 2007) collected Lake Becharof surface water at the main gas vent near The Gas Rocks and seeps on the ridge near Ukinrek Maars (Evans et al., 2007; their samples VH05 and VH10); Motyka (1977) collected Katmai Lake in two locations in 1975.

*Surface waters is an average of 46 samples from a large area of southeastern Alaska around Kaguyak, from $57^\circ 30'$ to 59° latitude and 153° to 157° longitude ($\sim 41,250 \text{ km}^2$) as reported in the U.S. Geological Survey National Water Information System (NWIS).

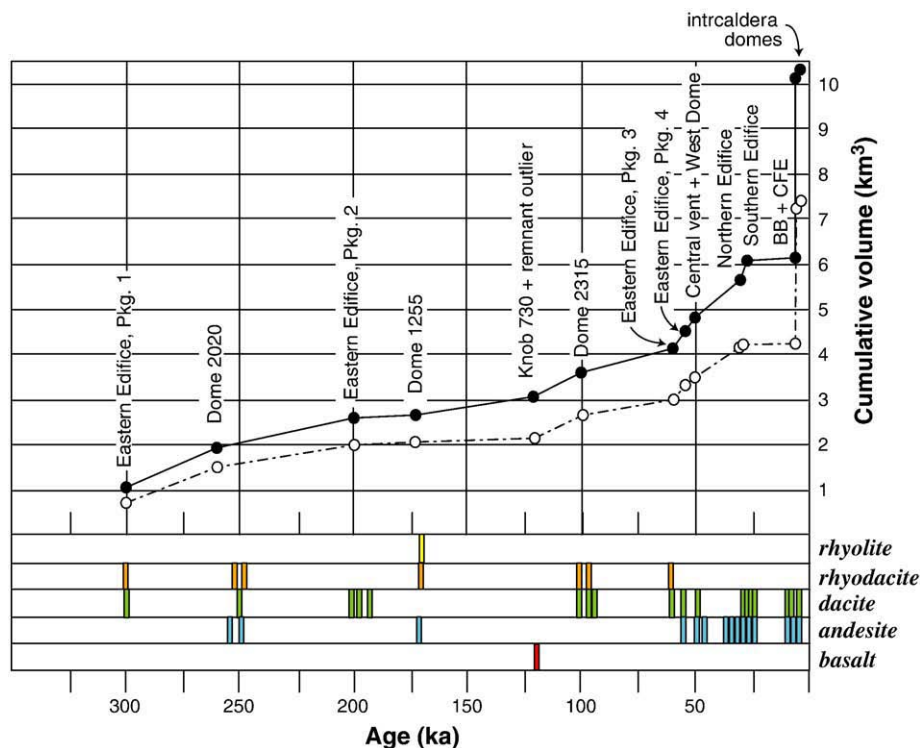


Fig. 23. Cumulative volume erupted through time at Kaguyak dome field, including the Holocene Big Breccia (BB) and caldera-forming eruption (CFE). Calculated minimums (open circles, dashed lines) and maximums (filled circles, solid lines) reflect preserved and pre-erosion volumes, respectively, as explained in text. Also shown are magma compositions erupted through time, colored as in Fig. 24.

dome complexes over intervals that probably lasted decades to millennia. Only the Eastern Edifice, which erupted intermittently over an interval of ~250 kyr, is represented on Fig. 23 as four separate eruptive packages, the second of which is poorly constrained in age.

Most notable from the cumulative curves is that volumetric output was moderately consistent for nearly 250 kyr until the rate increased by an order of magnitude between ~60 and 30 ka. Rhyodacite, dacite, and andesite erupted throughout, true rhyolite (74% SiO₂) only at 170 ka, and basaltic magma only once ~120 ka. Pre-Holocene cumulative volume, a modest 4–6 km³, nearly doubled during the short interval (probably days) of the caldera-forming eruption ~6 ka.

Most of the Kaguyak magma that erupted prior to the Holocene was intermediate in composition, over half dacitic and nearly 30% andesitic, with the remainder including as much as 12% rhyodacite, no more than 1% rhyolite, and no more than 6% basalt. The largely dacitic Holocene eruptions contributed only a trivial amount of andesite. The cumulative volume of 7 to 10 km³ for the entire center has proportions of at least 70% dacite, just under 20% andesite, 7% rhyodacite, less than 4% basalt and less than 1% rhyolite. The background eruptive rate for most of that time, between 300 and 60 ka, was 0.017 km³/k.y., which included emplacement of all of the extracaldera domes and two-thirds of the Eastern Edifice. In contrast, the dome-building rate during emplacement of the Central, Northern, Southern, and upper third of the Eastern Edifices (60–30 ka) was an order of magnitude larger at ~0.11 km³/k.y. Andesite, dacite, and rhyodacite have erupted repeatedly throughout the history of the volcanic field, with no apparent time-compositional trend except that rhyodacite has not erupted from the caldera-centered focus. Geographic distribution of the erupted compositions thus shows the SE quadrant to be, overall, more silicic than the rest of the field because it includes all the rhyodacitic units and the sole rhyolite. It does, however, also include the only erupted basalt (Fig. 24).

Perhaps most striking is the change in focus of activity from the distributed vent field active between 300 and 60 ka, to the

geographically more restricted vent field active between 60 and 30 ka (Fig. 24). Once the main eruptive focus moved ~2 km northwestward, the vents became more closely overlapping and the eruption rate greatly increased. Rhyodacites and low-TiO₂ magmas are absent in the northwesterly vent cluster, though they had been abundant eastward, prior to the 60-ka shift of focus. The only apparent exceptions to these geographic and chemical changes are the lavas of Package 4 from the Eastern Edifice, which apparently erupted ~1.5 km further east than the rest of the younger vents (just about on the present caldera rim), and the two andesite remnants north of Big River. All three plot along the low-TiO₂ trend of the Eastern Edifice, but none are well dated.

That the Holocene caldera coincides with the 60–30 ka vent cluster is probably not fortuitous. The Holocene Big Breccia and caldera-forming eruption deposits are the only substantial pyroclastics associated with the entire 300-kyr span of the Kaguyak dome field. It seems likely that sporadic eruption over 30 kyr of 1.5–2 km³ of precaldera magma from an area no larger than 3 km² represented the build-up of thermal and magmatic conditions leading to the caldera-forming eruption. Such a sequence of silicic dome growth followed by protracted quiescence (30 ka to 6 ka), then culmination in a large magnitude explosive eruption, is similar to that described at Bezymianny (Gorshkov, 1959), Katmai (Hildreth and Fierstein, 2000), and Mazama (Bacon and Lanphere, 2006).

Vents for the Holocene eruptive episodes, including both the Big Breccia (i.e., the inferred Southwest Dome) and the ignimbrite, were positioned over an area that had leaked compositionally similar dacitic magma during 10 of the 15 preceding eruptive events that built the Central, Western, and Southern Edifices. The Northern Edifice lavas plot separately only on account of being more mafic than the Holocene products; their compositional trends are collinear (Fig. 5). Although the Southern Edifice compositional trend is likewise mostly similar, slightly lower K₂O, Ba, and Zr values distinguish these dacites from the Holocene eruptives (Figs. 5, 14). Clasts from the Big Breccia

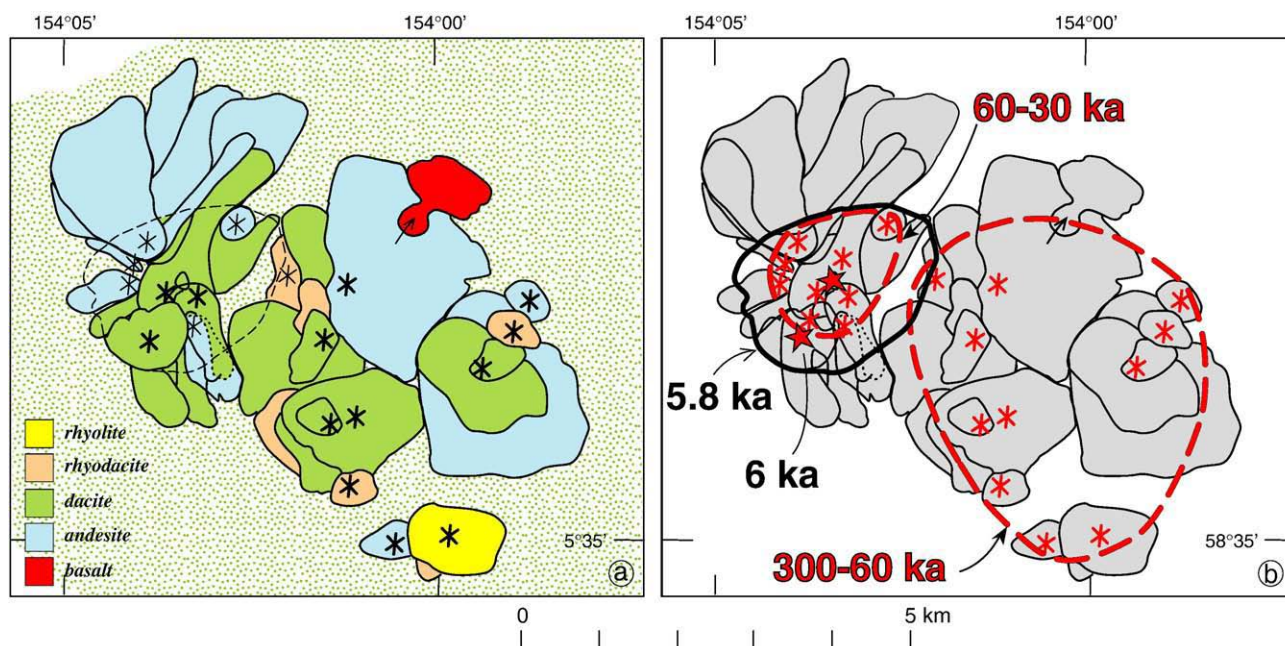


Fig. 24. (a) Geographic distribution of rhyolite, rhyodacite, dacite, andesite, and basalt domes and lava flows at Kaguyak 300 to 30 ka, prior to the Holocene caldera-forming event; lava compositions colored as in Fig. 23; present caldera rim dashed; vents marked by asterisks. (b) Eruptive focus from 300–60 ka was southeast of 60–30 ka eruptive focus (both foci outlined by dashed red lines); vents marked by red asterisks. All vents for eruptions 60–30 ka were within the area of the Holocene caldera (heavy black line). Post-caldera domes (vents marked by red stars) are also within the caldera. There was no older caldera, likely owing in part to wider geographic and temporal spacing of eruptions.

wholly overlap compositionally with the pumiceous ejecta of the ignimbrite and fallout that followed just a century or two later. The magma reservoir was not emptied by the caldera-forming eruption, as shown by the two chemically similar post-caldera domes that now protrude above the caldera lake.

13. Conclusions

Kaguyak has been active for at least 300 kyr and has erupted as much as 10 km³ of magma ranging from basalt (53% SiO₂) to rhyolite (74% SiO₂). Most activity has been viscous extrusion of domes and stubby exogenous flow lobes. There is evidence for only a few lava flows longer than 1 or 2 km. An especially active dome-building period between 60 and 30 ka was followed by a quiescent interval

more than 20 kyr long, which culminated in the caldera-forming eruption and its Big Breccia precursor. The caldera-forming eruption produced a moderate-sized ignimbrite and relatively small-volume subplinian fallout, permitting subsidence of a 2.5-km-wide caldera, and truncating the field of overlapping domes. The coignimbrite ash associated with the eruption was distributed at least as far as 80 km SW and 280 km NE.

Volumetrically, most of the eruptive products from Kaguyak are dacitic, with a significant fraction of andesitic lavas as well. Relatively less rhyodacite and only minor rhyolite and basalt were erupted here. Magma types include a low-TiO₂ suite (Eastern Edifice, Dome 2315, and outlier lavas), a minor high-TiO₂ suite (all from Dome 2020 cluster), and a TiO₂ suite between them that includes everything else. The entire Kaguyak suite is unusually low-K. It is, in fact, the lowest-K suite of which we are aware in the whole Aleutian Arc (Fig. 25). Only Augustine volcano approaches such low values of K₂O, but there is a spectrum spanning 1.5% K₂O among basalts alone along the length of the Aleutian Arc (Fig. 25). This characteristic is not strictly geographic, however; while Fourpeaked volcano (the next volcano NE of Kaguyak; Fig. 1) is also fairly low-K, its close neighbor, Mount Douglas, is not (Fig. 25).

Holocene explosive eruptions, two post-caldera domes, and continued gas bubbling through the 150-m-deep caldera lake, are evidence of the youth of this system. Kaguyak's history of dome growth and the not uncommon phenomenon elsewhere of rebuilding destroyed edifices by recurring dome extrusions, suggests that another dome-building episode through the caldera lake should not be unexpected.

Acknowledgements

This remote Alaskan fieldwork required logistical arrangements facilitated by many, including: Mike McKinnon (USGS, Alaska Volcano Observatory) for the loan of the boat used to map the caldera walls while we were camped on the island; John Paskievitch for helicopter logistics; King Salmon U.S. Fish and Wildlife Services for use of the bunkhouse; U.S. National Park Service for permitting geologic work in Katmai National Park and Preserve; and KatmaiAir and the derring-do of their pilots who landed us and our gear on the caldera lake.

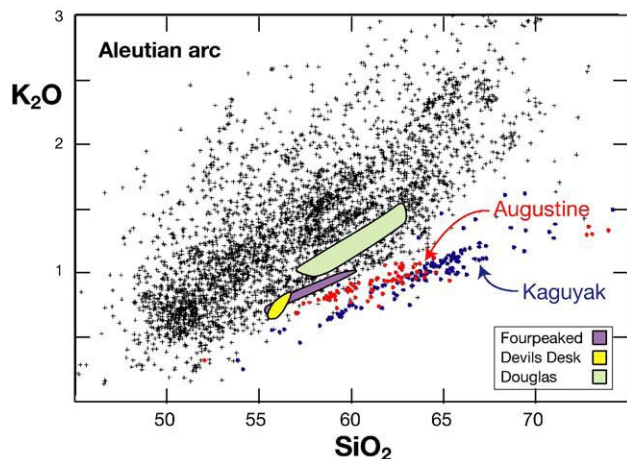


Fig. 25. K₂O vs. SiO₂ for all Aleutian arc volcanoes. Kaguyak is the lowest-K of all, with Augustine a close second. Fourpeaked and Devils Desk, ~25 km NE and SW of Kaguyak, respectively, also have moderately low values of K₂O, but others nearby do not. Kaguyak, Douglas and Fourpeaked data from this study; Devils Desk data from Hildreth et al. (2004); all others from Alaska Volcano Observatory database (Chris Nye, personal communication).

Helicopter pilot Jim Sink, notably calm and unflappable, added humor and good company to long commutes, and Dave Tucker, a stalwart field companion, added a large measure of wilderness competence and expert boat handling. Nicole Lautze, Tina Neal, Steve Self, and John Wolfe provided helpful reviews. We thank them all. Most chemical analyses were provided by the GeoAnalytical Laboratory of Washington State University and some by the USGS laboratory in Denver, CO. Radiocarbon ages were all determined at Geochron Laboratories in Cambridge, MA. K/Ar and $^{40}\text{Ar}/^{39}\text{Ar}$ dating was done by Andy Calvert in the U.S. Geological Survey Geochronology laboratory in Menlo Park, CA, and water from the Kaguyak Lake was analyzed by Cathy Janik, U.S. Geological Survey Geochemistry Laboratory in Menlo Park, CA.

Appendices A, B, C. Supplementary data

Supplementary data associated with this article can be found, in the online version, at doi:[10.1016/j.jvolgeores.2008.05.016](https://doi.org/10.1016/j.jvolgeores.2008.05.016).

References

- Adleman, J.N., 2005. Analysis of composition and chronology of dome emplacement at Black Peak Volcano, Alaska utilizing Aster remote sensing data and field-based studies: MS thesis, University of Alaska, Fairbanks.
- Allen, C.C., Jercinovic, M.J., Allen, J.S.B., 1982. Subglacial volcanism in north-central British Columbia and Iceland. *J. Geol.* 90, 699–715.
- Bacon, C.R., Metz, J., 1984. Magmatic inclusions in rhyolites, contaminated basalts, and compositional zonation beneath the Coso volcanic field, California. *Contrib. Mineral. Petrol.* 85, 346–365.
- Bacon, C.R., Lanphere, M., 2006. Eruptive history and geochronology of Mount Mazama and the Crater Lake region, Oregon. *Geol. Soc. Am. Bull.* 118, 1331–1359.
- Calvert, A., Lanphere, M.A., 2006. Argon geochronology of Kilauea's early submarine history. *J. Volcanol. Geotherm. Res.* 151, 1–18.
- Calvert, A., Fierstein, J., Hildreth, W., 2003. Silicic eruptions of the past 50 ka at the Three Sisters volcanic cluster, Oregon: EOS (American Geophysical Union Transactions) v. 84: no. 46.
- Cameron, W.A., Larson, G.L., 1992. Baseline inventory of the aquatic resources of Aniakchak National Monument, Alaska. National Park Service Technical Report 92/03: 243 p.
- Doe, B.R., Lipman, P.W., Hedge, C.E., Kurasawa, H., 1969. Primitive and contaminated basalts from the Southern Rocky Mountains, U.S.A. *Contrib. Mineral. Petrol.* 21, 142–156.
- Evans, W.C., Bergfeld, D., McGimsey, R.G., Hunt, A.G., 2007. Magmatic gas efflux at the Ukinrek Maars, Alaska. In: Bullen, T.D., Wang, Y. (Eds.), *Water–Rock Interactions* 12, v. 1. Taylor and Francis, London, pp. 65–69.
- Fierstein, J., 2007. Explosive eruptive record in the Katmai Region, Alaska Peninsula: an overview. *Bull. Volcanol.* 69, 469–509.
- Fierstein, J., Hildreth, W., 1992. The plinian eruptions of 1912 at Novarupta, Katmai National Park, Alaska. *Bull. Volcanol.* 54, 646–684.
- Fierstein, J., Nathenson, M., 1992. Another look at the calculation of fallout tephra volumes. *Bull. Volcanol.* 54, 156–167.
- Freundt, A., Schmincke, H.U., 1985. Lithic-enriched segregation bodies in pyroclastic flow deposits of Laacher See Volcano (East Eifel, Germany). *J. Volcanol. Geotherm. Res.* 25, 193–224.
- Gill, J.B., 1981. *Orogenic Andesites and Plate Tectonics*. Springer, Berlin Heidelberg New York, p. 390.
- Gorshkov, G.S., 1959. Gigantic eruption of the Volcano Bezymianny. *Bull. Volcanol.* 20, 77–109.
- Hildreth, W., Fierstein, J., 2000. Katmai volcanic cluster and the great eruption of 1912. *Geol. Soc. Am. Bull.* 112, 1594–1620.
- Hildreth, W., Fierstein, J., Siems, D.F., 2004. Rear-arc vs. arc-front volcanoes in the Katmai reach of the Alaska Peninsula: a critical appraisal of across-arc compositional variation. *Contrib. Mineral. Petrol.* 147, 243–275.
- Johnston, D.A., 1978. Volatiles, magma mixing, and the mechanism of eruption of Augustine Volcano, Alaska. PhD thesis, University of Washington.
- Lescinsky, D.T., Sisson, T.W., 1998. Ridge-forming, ice-bounded lava flows at Mount Rainier, Washington. *Geology* 26 (4), 351–354.
- Lipman, P.W., Mullineau, D.R., 1981. The 1980 eruptions of Mount St. Helens. Washington. US Geol. Surv., Prof. Paper 1250, 844.
- Mathews, W.H., 1947. "Tuyas," flat-topped volcanoes in northern British Columbia. *Am. J. Sci.* 245, 560–570.
- Motyka, R., 1977. Katmai caldera: glacier growth, lake rise, and geothermal activity. Short notes on Alaska geology. State of Alaska Div. Geol. and Geophys. Surv. Report 55, 17–21.
- Nowak, M., 1968. Archaeological dating by means of volcanic ash strata. PhD thesis, Department of Anthropology, University of Oregon, Eugene.
- Pinney, D.S., 1993. Late Quaternary glacial and volcanic stratigraphy near Windy Creek, Katmai National Park, Alaska. MSc thesis, University of Alaska, Fairbanks.
- Reger, R.D., Pinney, D.S., Burke, R.M., Wiltse, M.A., 1996. Catalog and initial analyses of geologic data related to Middle to Late Quaternary deposits, Cook Inlet Region, Alaska. State of Alaska. Div. Geol. and Geophys. Surv. Report 95–6, 188.
- Riehle, J.R., 1985. A reconnaissance of the major Holocene tephra deposits in the upper Cook Inlet region, Alaska. *J. Volcanol. Geotherm. Res.* 26, 37–74.
- Riehle, J.R., Dettmerman, R.L., Yount, M.E., Miller, J.W., 1994. Geologic map of the Mount Katmai quadrangle and adjacent parts of the Naknek and Afognak quadrangles, Alaska. U.S. Geological Survey Miscellaneous Investigations Series Map 1 2204, unpagged, 1 plate, scale 1:250,000.
- Riehle, J.R., Waitt, R.B., Meyer, C.E., Calk, L.C., 1996. Age of formation of Kaguyak Caldera, eastern Aleutian arc, Alaska, estimated by tephrochronology. *Geologic Studies in Alaska by the U.S. Geological Survey*.
- Riehle, J.R., Meyer, C.E., Miyaoka, R.T., 1999. Data on Holocene tephra (volcanic ash) deposits in the Alaska Peninsula and Lower Cook Inlet region of the Aleutian volcanic arc, Alaska. USGS Open-File Report 99–135 http://kiska.giseis.alaska.edu/dbases/akpen_tephra/akpen_tephra.html.
- Scott, W.E., Hoblitt, R.P., Torres, R.C., Self, S., Martinez, M.M.L., Nillos Jr., T., 1996. Pyroclastic flows of the June 15, 1991, climactic eruption of Mount Pinatubo. In: Newhall, C.G., Punongbayan, R.S. (Eds.), *Fire and Mud, Eruptions and Lahars of Mount Pinatubo, Philippines*. Univ. of Washington Press, Seattle, pp. 545–570.
- Symonds, R.B., Janik, C.J., Evans, W.C., Ritchie, B.E., Counce, D., Poreda, R.J., Iven, M., 2003. Scrubbing masks magmatic degassing during repose at Cascade-Range and Aleutian-Arc volcanoes. USGS Open-File Report 03-435.
- U. S. Geological Survey, National Water Information System, 2007. Water Data for the Nation. <http://nwis.waterdata.usgs.gov/nwis>.
- Walker, G.P.L., 1971. Grain-size characteristics of pyroclastic deposits. *J. Geol.* 79, 696–714.
- Webb, R.W., 1941. Quartz xenocrysts in olivine basalt from the Southern Sierra Nevada of California. *Am. Mineral.* 26, 321–337.
- Wood, C.A., Kienle, J., 1990. *Volcanoes of North America*. Cambridge University Press, New York, pp. 75–77.